Available online at www.sciencedirect.com
ScienceDirect
International Journal of Heat and Mass Transfer 50 (2007) 3122–3140
International Journal of HEAT and MASS TRANSFER
www.elsevier.com/locate/ijhmt

Nonlinear thermohaline convection in rotating fluids

S.G. Tagare [a], M.V. Ramana Murthy [b], Y. Rameshwar [c,*]

[a] Department of Mathematics, Addis Ababa University, Addis Ababa, P.O. Box 1176, Ethiopia
[b] Department of Mathematics, Osmania University, Hyderabad 500 007, India
[c] Department of Mathematics, P.G. College of Science, Saifabad, Hyderabad 500 004, India

Received 25 December 2005; received in revised form 17 July 2006
Available online 21 March 2007

Abstract

Linear and weakly nonlinear properties of thermohaline convection in rotating fluids are investigated. Linear stability analysis is studied by plotting graphs for different values of physical parameters relevant to the Earth's outer core and oceans. We have derived a nonlinear two-dimensional Landau–Ginzburg equation with real coefficients near the onset of stationary convection at the supercritical pitchfork bifurcation and shown the occurrence of Eckhaus and zigzag instabilities. We have studied heat transfer by using Nusselt number which is obtained from Landau–Ginzburg equation at the onset of stationary convection for the steady case. A coupled two-dimensional Landau–Ginzburg type equations with complex coefficients near the onset of oscillatory convection are derived and the stability regions of travelling and standing waves discussed.

Keywords: Thermohaline convection; Bifurcation points; Nusselt number; Travelling and standing wave convection and secondary instabilities

1. Introduction

The understanding of convection in rotating fluids is of fundamental importance in many problems of geophysical and astrophysical fluid dynamics. Thermohaline convection in rotating system is one of the reason for mixing of different masses of water in oceans, mixing of light alloying elements like Sulphur in molten Iron in Earth's outer core and mixing of Helium (which is formed due to fusion of Hydrogen) in Hydrogen in stellar core.

Thermohaline convection, convection in binary liquid and magnetoconvection are examples of double diffusive system. In thermohaline convection, the temperature and the salt concentration provide the two diffusivities. Convection in binary liquids is similar to the thermohaline convection except for the fact that a temperature difference can drive a mass current. In convection in binary liquids, the temperature and the concentration of the light component of the liquid provide two diffusivities. These convective double diffusive systems and Rayleigh–Benard convection in rotating fluid are capable of showing stationary convection at pitchfork bifurcation, oscillatory convection at Hopf bifurcation (both these bifurcations are primary bifurcations), Takens–Bogdanov bifurcation and co-dimension two bifurcation (these two bifurcations are secondary bifurcations).

In this paper, we study thermohaline convection in rotating fluid (which is kept rotating at a constant angular velocity $\vec{\Omega} = \Omega\hat{e}_z$, about z-axis) lying between two horizontal boundaries which are dynamically free. The onset of instabilities in rotating thermohaline convection has been considered by Pearlistein [6]. The problem where the Taylor number is chosen so that there is a triple zero eigenvalue (corresponding to a bifurcation point of co-dimension three) has been investigated for rotating thermohaline convection by Arneodo et al. [1]. The onset of instabilities in rotating magnetoconvection for viscous fluid has been investigated by Tagare [7] and for inviscid fluid has been investigated by Tagare and Rameshwar [8].

In Section 2, we write basic equations of thermohaline convection in rotating fluid. In Section 3, we study the

* Corresponding author. Tel.: +91 40 2455 3346.
E-mail address: yrhwr@yahoo.com (Y. Rameshwar).

0017-9310/$ - see front matter © 2007 Elsevier Ltd. All rights reserved.
doi:10.1016/j.ijheatmasstransfer.2006.11.037

Nomenclature

A_{1L}	amplitude of left travelling waves
A_{1R}	amplitude of right travelling waves
C	perturbed concentration
d	vertical length scale
g	gravitational acceleration
H	rate of heat transport
L	Lewis number
Nu	Nusselt number
P'	pressure
p	growth rate of disturbances
Pr	Prandtl number
q	horizontal wave number
R_1	thermal Rayleigh number
R_2	salinity Rayleigh number
S'	salinity concentration
$\Delta S'$	salinity concentration between upper and lower layers
t	time coordinate
Ta	Taylor number
T'	temperature
$\Delta T'$	temperature difference between upper and lower layers
u, v, w	horizontal and vertical velocity components
x, y, z	horizontal and vertical coordinates

Greek symbols

ρ', ρ'_o	density and mean density of the fluid
ν	kinematic viscosity
κ_T, κ_S	thermal diffusivity and salinity diffusivity
Ω	angular velocity
α, β_s	thermal and salinity expansion coefficients
ω	frequency

Superscript

$'$	variables with dimension

linear stability analysis. Since the bifurcation is continuous one, only a slow modulation of the convective roll pattern is allowed by the fluid equations near the onset. The time evolution of general pattern is developed in Section 4, for a region $R_2 < R_{2c}$, (where $R_2 = R_{2c}$ corresponds to a critical value of the salinity Rayleigh number in a rotating thermohaline convection at a Takens–Bogdanov bifurcation point) by means of multiple scale analysis used by Newell and Whitehead [5]. In Section 4, we derive a nonlinear two-dimensional Landau–Ginzburg equation in a complex amplitude $A(X, Y, T)$ with real coefficients. In Section 4.1, we have shown the occurrence of secondary instabilities such as Eckhaus instability and zigzag instability. In Section 4.2, by dropping t-dependence from stationary Landau–Ginzburg equation we have studied Nusselt number at the lower plate. In Section 5, we derive coupled Landau–Ginzburg type equations in complex amplitudes A_{1R}, A_{1L} with complex coefficients. Here A_{1R} and A_{1L} stand for amplitudes of right hand and left hand travelling waves. When $A_{1R} = A_{1L}$, we get standing waves. In Section 5.1, following Matthews and Rucklidge [4], we have dropped slow space dependence and obtained two ordinary differential equations in $A_{1R}(T), A_{1L}(T)$, with complex coefficients, termed as Landau equations and discussed the stability regions of travelling waves and standing waves. We have given exact analytical solutions for the complex Landau equations. In Section 6, we write the conclusions of this paper.

2. Basic equations

We consider an infinite horizontal layer of fluid of depth d with linear temperature and salinity gradient (in the undisturbed state) which is kept rotating at a constant angular velocity $\vec{\Omega} = \Omega\hat{e}_z$ about z-axis. Following Veronis [9], we consider density ρ' as

$$\rho' = \rho'_o[1 - \alpha(T' - T'_b) + \beta_s(S' - S'_b)], \tag{2.1}$$

where ρ'_o is the mean density of the system, T' and S' are the temperature and salinity concentration of the system. α and β_s are thermal and salinity expansion coefficients of density with respect to temperature and concentration. Here $\alpha > 0,\ \beta_s > 0$ in oceanic water because density of salt is more than water. In Earth's outer core $\beta_s < 0$ because density of liquid Iron (which acts like main liquid in thermohaline convection) is more than molten Sulphur (which acts like salt). In oceanic fluid, temperature gradient is destabilizing and salinity gradient is stabilizing. In Earth's outer core both temperature and salinity gradients are destabilizing. However, rotation is always stabilizing. Thermohaline convection in rotating fluid is an example of triple diffusive system. We use Cartesian system of co-ordinates whose dimension co-ordinates x', y' and z' are scaled on d. The velocity vector $\vec{V}(u', v', w')$, density ρ', temperature θ', salinity concentration C', time t' and pressure P' are non-dimensionalised by scales κ_T/d, ρ'_o, $\Delta T'$, $\Delta S'$, d^2/κ_T and $\rho'_o\kappa_T d^2$. In the Boussinesq approximation one considers the fluid incompressible except when dealing with the buoyancy terms which drives the thermal and salinity concentration. The dimensionless parameters required for the description of the motion are: thermal Rayleigh number $R_1 = \alpha g\Delta T' d^3/\kappa_T\nu$, salinity Rayleigh number $R_2 = \beta_s g\Delta S' d^3/\ \kappa_T\nu$, Taylor number $Ta = 4\Omega^2 d^4/\nu^2$, thermal Prandtl number $Pr = \nu/\kappa_T$, Lewis number $L = \kappa_S/\kappa_T < 1$. This implies that heat diffusive is faster than salt. The basic dimensionless equations for thermohaline convection in a rotating fluid in the Boussinesq approximation are:

$$\nabla \cdot \vec{V} = 0, \tag{2.2}$$

$$\frac{1}{Pr}\left[\frac{\partial \vec{V}}{\partial t} + (\vec{V}\cdot\nabla)\vec{V}\right] = -\nabla\left(\frac{p_1}{Pr} - \frac{PrTa}{8}|\vec{\Omega}\times\vec{r}|^2\right) + \nabla^2\vec{V} + Ta^{\frac{1}{2}}(\vec{V}\times\vec{\Omega}) + (R_1\theta - R_2C)\hat{e}_z, \tag{2.3}$$

$$\frac{\partial\theta}{\partial t} + (\vec{V}.\nabla)\theta = w + \nabla^2\theta, \tag{2.4}$$

$$\frac{1}{L}\left[\frac{\partial C}{\partial t} + (\vec{V}.\nabla)C\right] = \frac{w}{L} + \nabla^2 C. \tag{2.5}$$

The curl of Eq. (2.3) gives

$$\left(\frac{1}{Pr}\frac{\partial}{\partial t} - \nabla^2\right)\nabla\times\vec{V} - Ta^{\frac{1}{2}}\nabla\times(\vec{V}\times\hat{e}_z) - \nabla[R_1(\theta\hat{e}_z) - R_2(C\hat{e}_z)] = -\frac{1}{Pr}\nabla\times[(\vec{V}.\nabla)\vec{V}], \tag{2.6}$$

where the vorticity $\vec{\omega} = \nabla\times\vec{V} = (\omega_x, \omega_y, \omega_z)$. The z-component of Eq. (2.6) and the z-component of curl of Eq. (2.6) give

$$\left(\frac{1}{Pr}\frac{\partial}{\partial t} - \nabla^2\right)\omega_z = Ta^{\frac{1}{2}}\frac{\partial w}{\partial z} - \frac{1}{Pr}[(\vec{V}\cdot\nabla)\omega_z - (\vec{\omega}\cdot\nabla)w], \tag{2.7}$$

$$\left(\frac{1}{Pr}\frac{\partial}{\partial t} - \nabla^2\right)\nabla^2 w - \nabla_h^2(R_1\theta - R_2C) + Ta^{\frac{1}{2}}\frac{\partial\omega_z}{\partial z} = \frac{1}{Pr}\hat{e}_z\cdot[(\vec{V}\cdot\nabla)\vec{\omega} - (\vec{\omega}\cdot\nabla)\vec{V}], \tag{2.8}$$

where $\nabla_h^2 = \partial^2/\partial x^2 + \partial^2/\partial y^2$ is the horizontal operator. Eliminating θ, C, ω_z from Eqs. (2.4), (2.5), (2.7) and (2.8), we get

$$\mathscr{L}w = \mathscr{N}, \tag{2.9}$$

where

$$\mathscr{L} = \left(\frac{\partial}{\partial t} - \nabla^2\right)\left(\frac{1}{L}\frac{\partial}{\partial t} - \nabla^2\right)\left[\left(\frac{1}{Pr}\frac{\partial}{\partial t} - \nabla^2\right)^2\nabla^2 + Ta\frac{\partial^2}{\partial z^2}\right] - R_1\nabla_h^2\left(\frac{1}{Pr}\frac{\partial}{\partial t} - \nabla^2\right)\left(\frac{1}{L}\frac{\partial}{\partial t} - \nabla^2\right) + \frac{R_2}{L}\nabla_h^2\left(\frac{1}{Pr}\frac{\partial}{\partial t} - \nabla^2\right)\left(\frac{\partial}{\partial t} - \nabla^2\right), \tag{2.10}$$

$$\begin{aligned}\mathscr{N} = &-R_1\nabla_h^2\left(\frac{1}{Pr}\frac{\partial}{\partial t} - \nabla^2\right)\left(\frac{1}{L}\frac{\partial}{\partial t} - \nabla^2\right)(\vec{V}\cdot\nabla)\theta \\ &+ \frac{R_2}{L}\nabla_h^2\left(\frac{1}{Pr}\frac{\partial}{\partial t} - \nabla^2\right)(\vec{V}\cdot\nabla)C \\ &+ \frac{1}{Pr}\left(\frac{1}{L}\frac{\partial}{\partial t} - \nabla^2\right)\left(\frac{\partial}{\partial t} - \nabla^2\right)\hat{e}_z\cdot\{\nabla\times[(\vec{V}\cdot\nabla)\vec{\omega} - (\vec{\omega}\cdot\nabla)\vec{V}]\} \\ &+ \frac{Ta^{\frac{1}{2}}}{Pr}\left(\frac{1}{L}\frac{\partial}{\partial t} - \nabla^2\right)\left(\frac{\partial}{\partial t} - \nabla^2\right)\frac{\partial}{\partial z}[(\vec{V}\cdot\nabla)\omega_z - (\vec{\omega}\cdot\nabla)w].\end{aligned} \tag{2.11}$$

3. Linear stability analysis

We perform the linear stability analysis of the problem by substituting

$$w = W(z)e^{(iqx+pt)}$$

into linearized version of Eq. (2.9) viz. $\mathscr{L}w = 0$, and obtaining equation

$$\begin{aligned}&(D^2 - q^2 - p)\left(D^2 - q^2 - \frac{p}{L}\right)\times\left[(D^2 - q^2)\left(D^2 - q^2 - \frac{p}{Pr}\right)^2 + TaD^2\right]W \\ &= -q^2\left(D^2 - q^2 - \frac{p}{Pr}\right)\times\left[R_1\left(D^2 - q^2 - \frac{p}{L}\right) - \frac{R_2}{L}(D^2 - q^2 - p)\right]W,\end{aligned} \tag{3.1}$$

where $D = d/dz$ and p is the growth rate of the disturbances. In this paper we consider idealized free–free boundary conditions. Here W and all its even derivatives vanish at $z = 0$ and $z = 1$.

3.1. Determination of marginal stability when Rayleigh number R_1 is a dependent variable

Substituting $W(z) = \sin\pi z$ and $p = i\omega$ into Eq. (3.1), we get

$$R_1 = \frac{R_2\left(\varpi^4 + \frac{\omega^2}{L}\right)}{L\left(\varpi^4 + \frac{\omega^2}{L^2}\right)} + \frac{1}{q^2}\left[\varpi^2\left(\varpi^4 - \frac{\omega^2}{Pr}\right) + \frac{Ta\pi^2\left(\varpi^4 + \frac{\omega^2}{Pr}\right)}{\left(\varpi^4 + \frac{\omega^2}{Pr^2}\right)}\right] + i\omega\varpi^2(A_1\omega^4 + A_2\omega^2 + A_3), \tag{3.2}$$

where $\varpi^2 = \pi^2 + q^2$

$$A_1 = \frac{\varpi^2}{q^2L^2Pr^2}\left(1 + \frac{1}{Pr}\right), \tag{3.3a}$$

$$A_2 = \frac{\varpi^6}{q^2}\left(1 + \frac{1}{Pr}\right)\left(\frac{1}{L^2} + \frac{1}{Pr^2}\right) + \frac{R_2\left(1 - \frac{1}{L}\right)}{LPr^2} + \frac{Ta\pi^2}{L^2q^2}\left(1 - \frac{1}{Pr}\right), \tag{3.3b}$$

$$A_3 = \frac{\varpi^{10}\left(1 + \frac{1}{Pr}\right)}{q^2} + \frac{R_2\varpi^4}{L}\left(1 - \frac{1}{L}\right) + \frac{Ta\pi^2\varpi^4\left(1 - \frac{1}{Pr}\right)}{q^2}. \tag{3.3c}$$

From relation (3.3a), $A_1 > 0$, since $Pr > 0$. In this section, we obtain threshold Rayleigh numbers for the stationary instability and oscillatory instability.

3.1.1. Stationary convection ($\omega = 0$)

For the onset of stationary convection we set $\omega = 0$ into Eq. (3.2), we get

$$R_{1s} = \frac{R_2}{L} + \frac{(\varpi_s^6 + Ta\pi^2)}{q_s^2}. \tag{3.4}$$

Here R_{1s} is the value of Rayleigh number R_1 for the stationary convection. The critical value of R_{1s} is obtained for $q = q_{sc}$ where

$$2\left(\frac{q_{sc}}{\pi}\right)^6 + 3\left(\frac{q_{sc}}{\pi}\right)^4 = 1 + \frac{Ta}{\pi^4}. \tag{3.5}$$

Threshold for the onset of stationary convection at pitchfork bifurcation is given by Eq. (3.4), with $q = q_{sc}$. Thus

$$R_{1sc} = \frac{R_2}{L} + \frac{\varpi_{sc}^6 + Ta\pi^2}{q_{sc}^2}, \tag{3.6}$$

where $\varpi_{sc}^2 = \pi^2 + q_{sc}^2$. On eliminating Ta from Eqs. (3.5) and (3.6), we get

$$R_{1sc} = \frac{R_2}{L} + 3\varpi_{sc}^4.$$

3.1.2. Oscillatory convection ($\omega^2 > 0$)

For the oscillatory convection ($\omega \neq 0$) and from Eq. (3.2), R_1 will be complex. But the physical meaning of R_1 requires it to be real. The condition that R_1 is real implies that imaginary part of Eq. (3.2) is zero. That is

$$A_1\omega^4 + A_2\omega^2 + A_3 = 0, \tag{3.7}$$

where A_1, A_2, A_3 are given by Eqs. (3.3a)–(3.3c). We get $A_2 < 0$ and $A_3 > 0$, for $L < Pr < 1$ or $L > Pr > 1$ and for some values of other physical parameters. When $A_2 < 0$, $A_3 > 0$ according to Descarte's rule their exist two positive roots of Eq. (3.7), which are correspond to two onset frequencies. From $A_3 = 0$ we get

$$q^6 + 3\pi^2 q^4 + \left[3\pi^4 + \frac{R_2\left(1-\frac{1}{L}\right)}{L\left(1+\frac{1}{Pr}\right)}\right]q^2 + \frac{Ta\pi^2\left(1-\frac{1}{Pr}\right)}{\left(1+\frac{1}{Pr}\right)} + \pi^6 = 0. \tag{3.8}$$

We get two positive roots of Eq. (3.8) only when $R_2 > 0$. Oscillatory convection exist if atleast one root of Eq. (3.8) is positive. Critical wave number for stationary convection is depends on only Ta, but critical wave number of oscillatory convection depends on Ta, R_2, L and Pr. Each positive root of Eq. (3.8) corresponds to the Takens–Bogdanov bifurcation point. Takens–Bogdanov bifurcation point is the point at which the oscillatory neutral curve intersect the stationary neutral curve and the frequency on the oscillatory neutral curve approaches to zero as the intersection point is approached. Takens–Bogdanov bifurcation point corresponds to a double zero eigenvalue of the linear growth rate. At Takens–Bogdanov bifurcation point we get

$$R_{1s}(q_s) = R_{1o}(q_o) = R_{1c}(q_c) \quad \text{and} \quad q_s = q_o = q_c. \tag{3.9}$$

At the co-dimension two bifurcation point, we have

$$R_{1sc}(q_{sc}) = R_{1oc}(q_{oc}) \quad \text{and} \quad q_{sc} \neq q_{oc}. \tag{3.10}$$

Figs. 1–3 are plotted in (q, R_1)-plane. In Figs. 1–3, stationary convection thermal Rayleigh numbers are taken on solid lines and oscillatory convection thermal Rayleigh numbers are taken on dotted lines. In Figs. 1–3, we have observed the effect of physical parameters viz. Ta, R_2 and Pr on the onset of both stationary convection (pitchfork bifurcation) and oscillatory convection (Hopf bifurcation). These Figs. 1–3 show that when a parameter increases for the remaining fixed parameters the onset of both stationary convection and oscillatory convection increases. In Fig. 3, Prandtl number do not show any effect on the stationary convection, since stationary convection Rayleigh number R_{1s} is independent of Prandtl number. Fig. 3b shows both primary and secondary bifurcations. Fig. 4 is plotted in (R_2, R_1) plane. In Fig. 4a, the intersection point of a solid line and a dotted line appears at

$$R_2 = R_{2c} = \frac{L^2\left[\left(1+\frac{1}{Pr}\right)\varpi_c^6 + Ta\pi^2\left(1-\frac{1}{Pr}\right)\right]}{(1-L)q_c^2} \tag{3.11}$$

corresponding to a Takens–Bogdanov bifurcation point. In the limit $R_2 \to R_{2c}$, the frequency of the oscillatory instability tends to zero and weakly nonlinear analysis in this region gives us a nonlinear equation describes the behavior of the system near the Takens–Bogdanov bifurcation point. This Takens–Bogdanov bifurcation point increases as Taylor number increases. In Fig. 4b, the intersection point of a solid line and a dotted line corresponding to a Taylor number gives a co-dimension two bifurcation point. Let $R_2 = R_{2ct}$ at a co-dimension two bifurcation point. If $R_2 < R_{2ct}$, we get stationary convection as a first instability. If $R_2 > R_{2ct}$, then we get oscillatory convection as a first instability. Co-dimension two bifurcation point increases as Taylor number increases.

3.2. Determination of marginal stability when Rayleigh number R_1 is an independent variable

Substituting $W = \sin \pi z$ into Eq. (3.1), we get a fourth degree polynomial equation in p of the form

$$p^4 + Bp^3 + Cp^2 + Dp + E = 0, \tag{3.12}$$

where

$$B = \varpi^2(1 + L + 2Pr), \tag{3.13a}$$

$$C = \varpi^4[L(1+2Pr) + Pr(2+Pr)] + \frac{Ta\pi^2 Pr^2}{\varpi^2} - \frac{q^2 Pr}{\varpi^2}(R_1 - R_2), \tag{3.13b}$$

$$D = Pr[\varpi^6(Pr + 2L + LPr) + Ta\pi^2 Pr(1+L) - R_1 q^2(L+Pr) + R_2 q^2(1+Pr)], \tag{3.13c}$$

$$E = Pr^2\varpi^2[L(\varpi^6 + Ta\pi^2) + q^2(R_2 - R_1 L)]. \tag{3.13d}$$

Setting $p = i\omega$ in Eq. (3.12), and considering its real and imaginary parts, we get

$$\omega^4 - C\omega^2 + E = 0, \tag{3.14a}$$

$$B\omega^2 - D = 0. \tag{3.14b}$$

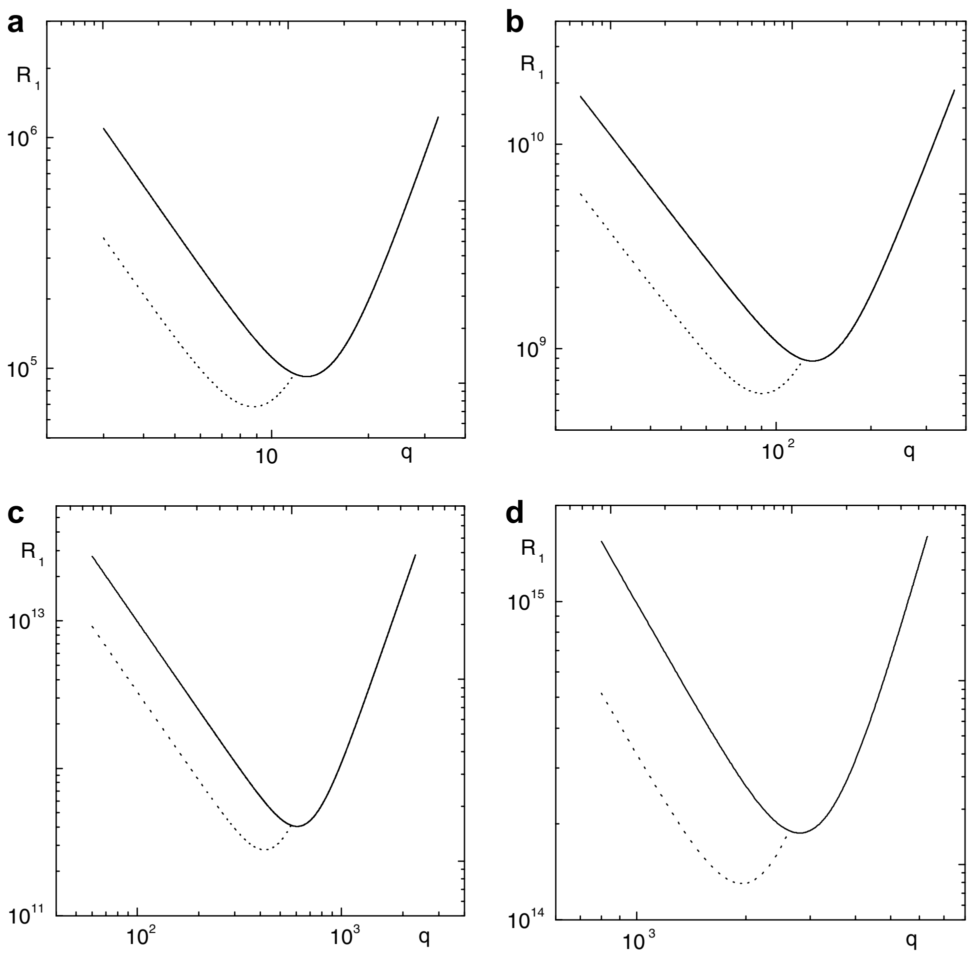

Fig. 1. Marginal stability curves (stationary convection – solid lines, oscillatory convection – dotted lines) are plotted for $Pr = 0.5$, $L = 0.1$, $R_2 = -0.5$ and (a) $Ta = 10^6$, (b) $Ta = 10^{12}$, (c) $Ta = 10^{16}$, (d) $Ta = 10^{20}$.

3.2.1. Stationary convection ($\omega = 0$)

Substituting $\omega = 0$ into Eq. (3.12), we get $E = 0$ which gives stationary convection. R_{1s} is determined by putting $R_1 = R_{1s}$ into $E = 0$. Let $s = q^2 (> 0)$, then the equation $E = 0$ can be written as

$$\left(R_1 - \frac{R_2}{L}\right)s = (s + \pi^2)^3 + Ta\pi^2. \tag{3.15}$$

We have given an analytical expression (3.6) to find critical thermal Rayleigh number by considering R_1 as a dependent variable. Similarly we can find an analytical expression for critical Taylor number by considering R_1 as an independent variable [3]. This critical Taylor number is computed as follows:

The derivative of Eq. (3.15) gives

$$R_1 - \frac{R_2}{L} = 3(s + \pi^2)^2. \tag{3.16}$$

Substituting $R_1 - (R_2/L)$ from Eq. (3.16) into Eq. (3.15), we get

$$2\left(\frac{s}{\pi^2}\right)^3 + 3\left(\frac{s}{\pi^2}\right)^2 = 1 + \frac{Ta}{\pi^2}. \tag{3.17}$$

Eq. (3.17) is nothing but Eq. (3.5), since $s = q^2$. Eq. (3.16) can be written in terms of s as

$$s = \left(\frac{R_1 - (R_2/L)}{3}\right)^{\frac{1}{2}} - \pi^2. \tag{3.18}$$

We consider only positive values of s. On substituting Eq. (3.18) into Eq. (3.15), we get the critical Taylor number $Ta = Ta_{sc}$ where

$$Ta_{sc} = \left(R_1 - \frac{R_2}{L}\right)\left[\left(\frac{R_1 - (R_2/L)}{R_{1rb}}\right)^{\frac{1}{2}} - 1\right] \quad \text{and} \quad R_{1rb} = \frac{27\pi^4}{4}. \tag{3.19}$$

Here R_{1rb} is the critical thermal Rayleigh number of Rayleigh–Bénard convection problem. From Eq. (3.19) we calculate critical Taylor number for the given parameters R_1, L and R_2. For the points $\{R_1, Ta_{sc}\}$ on the curve (3.19), $E = 0$ with

$$q = q_{sc} = \left[\left(\frac{R_1 - (R_2/L)}{3}\right)^{\frac{1}{2}} - \pi^2\right]^{\frac{1}{2}}. \tag{3.20}$$

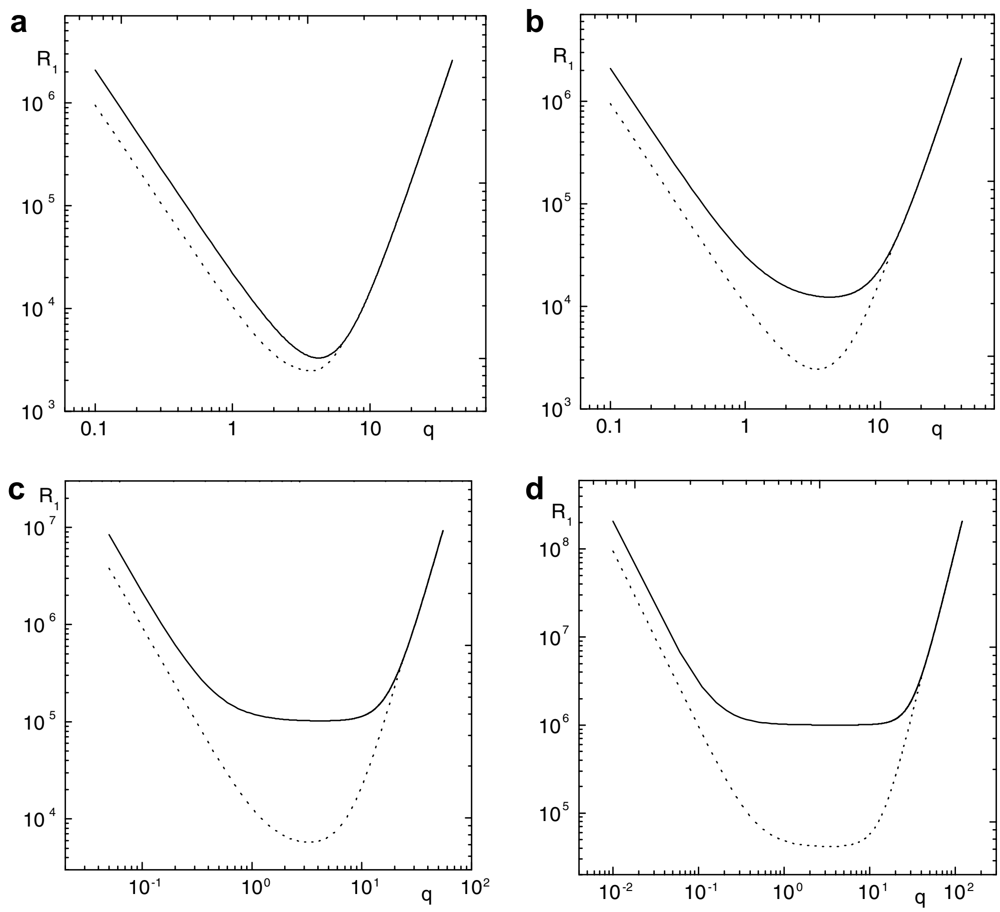

Fig. 2. Marginal stability curves (stationary convection – solid lines, oscillatory convection – dotted lines) are plotted for $Pr = 0.5,\ L = 0.1,\ Ta = 2000$ and (a) $R_2 = 10^3$, (b) $R_2 = 10^4$, (c) $R_2 = 10^5$, (d) $R_2 = 10^6$.

We have to use Eq. (3.20) to determine the sign of E (i.e., $E < 0,\ E > 0$). Here the system is stable for $E > 0$ ($R_1 < R_{1sc}$ for all s) and it is unstable for $E < 0$ ($R_1 > R_{1sc}$ in some range of s, i.e., $s_1 < s < s_2$). Fig. 5 is plotted in (R_1, Ta) plane for the curve (3.19). In this figure $Ta = 0$ on R_1 axis. On R_1 axis each solid line corresponds to R_2 starting from $R_1 = R_{1rb} + (R_2/L)$. The frequency $\omega = 0$ and $E = 0$ are conditions for pitchfork bifurcation corresponding to stationary convection.

3.2.2. Oscillatory convection ($\omega^2 > 0$)

From Eq. (3.14a), we can have marginal stability if $\omega^2 = D/B$, $D > 0$ and

$$D^2 - BCD + B^2E = 0. \tag{3.21}$$

Eq. (3.21) gives a quadratic equation in R_1. We will get oscillatory convection for a set of physical parameters corresponding to positive value of ω^2 and thermal Rayleigh number exists for $\omega^2 > 0$. Because of complicated expressions it is not possible to find closed forms for critical Taylor number and critical wave number of oscillatory convection.

At Takens–Bogdanov bifurcation point we get $\omega^2 = 0$, which gives $D = 0$ and $E = 0$. Eliminating Ta from $D = 0$ and $E = 0$, we get

$$q^6 + 3\pi^2 q^4 + \left[\frac{R_1(Pr-1)}{2} + \frac{R_2(L-Pr)}{2L^2} + 3\pi^4\right] q^2 + \pi^6 = 0. \tag{3.22}$$

Above Eq. (3.22) gives either two positive roots or no positive roots. We get two positive roots when $R_2 < 0$ and $Pr < L < 1$ or when $R_2 > 0$ and $L < Pr < 1$ (see Fig. 6). If the roots of Eq. (3.22) are positive then we get two Takens–Bogdanov bifurcation points. In Figs. 7 and 8 left side of the solid line below the intersection point and left side of the dotted line above the intersection point gives stability region of the system. In this stability region we get $D > 0$ and $D^2 - BCD + B^2E > 0$. In these Figs. 7 and 8 at the intersection point we get $\omega^2 > 0$, which gives co-dimension two bifurcation point. This co-dimension two bifurcation point moves down wards when Pr decreases in Figs. 7 and 8. Eliminating Ta and R_1 from equations $E = 0$, $D = 0$ and $C = 0$, we get

$$R_2 = R^*_{2c} = \frac{\varpi^6 L^3(1+2Pr)}{Prq^2(L-1)(Pr-L)}, \tag{3.23}$$

which is a co-dimension three bifurcation point corresponding to triple zero eigenvalue. In this paper we are considering physically realistic case of $L < 1$.

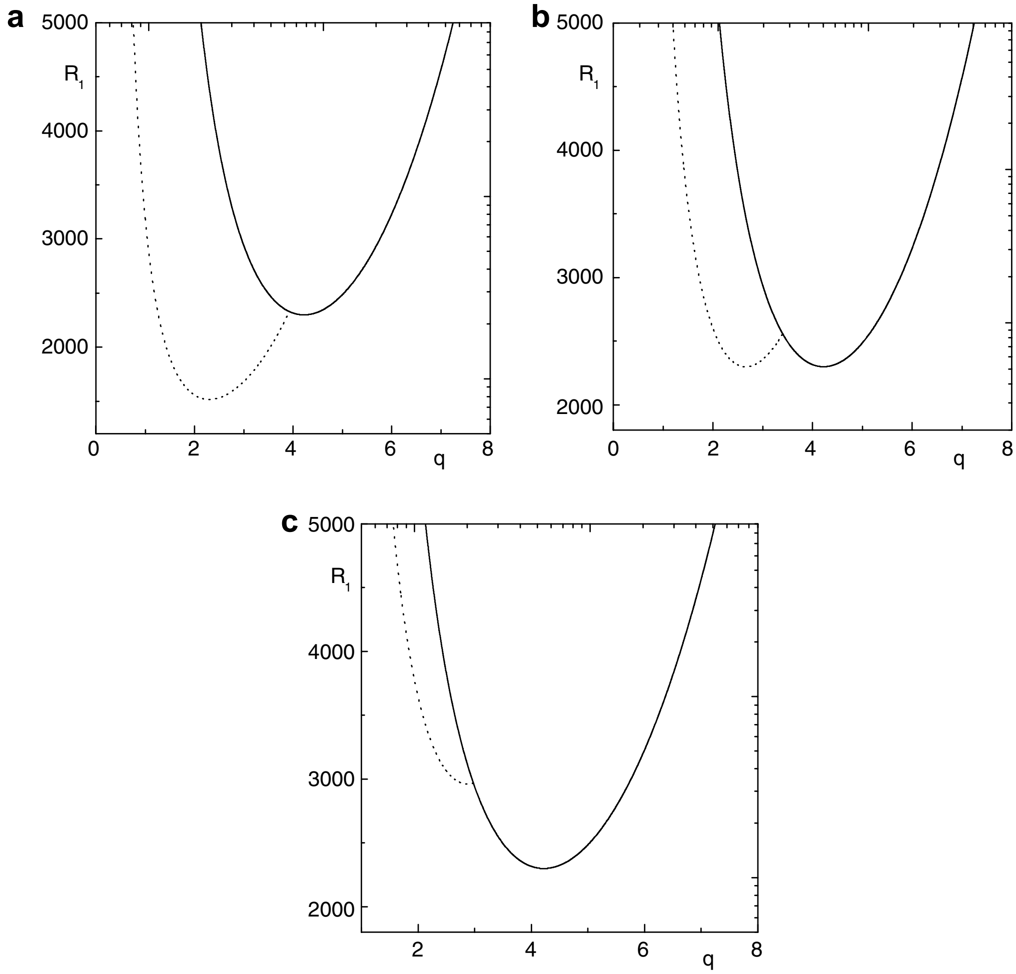

Fig. 3. Marginal stability curves (stationary convection – solid lines, oscillatory convection – dotted lines) are plotted for $Ta = 2000$, $L = 0.1$, $R_2 = -0.5$ and (a) $Pr = 0.025$, (b) $Pr = 0.33327$, (c) $Pr = 0.5$.

However for $L = 1$, we get the interesting results. At this value $L = 1$, Eq. (3.21) gives

$$(s+\pi^2)^3 + \frac{(R_2-R_1)s}{2(1+Pr)} + \frac{Ta\pi^2 Pr^2}{(1+Pr)^2} = 0. \tag{3.24}$$

Equations (3.15), (3.18) and (3.19) with $L = 1$ gives

$$(R_1-R_2)s = (s+\pi^2)^3 + Ta\pi^2, \tag{3.25}$$

$$s = \left(\frac{R_1-R_2}{3}\right)^{\frac{1}{2}} - \pi^2, \tag{3.26}$$

$$Ta_{sc} = (R_1-R_2)\left[\left(\frac{R_1-R_2}{R_{1rb}}\right)^{\frac{1}{2}} - 1\right]. \tag{3.27}$$

From Eq. (3.24), we can obtain critical wave number and critical Taylor number. On comparing Eqs. (3.24) and (3.25), and substituting

$$R_1 \to \frac{R_1}{2(1+Pr)}, \quad R_2 \to \frac{R_2}{2(1+Pr)}, \quad Ta \to \frac{TaPr^2}{(1+Pr)^2}, \tag{3.28}$$

into Eqs. (3.26) and (3.27), we get critical wave number q_{oc} and critical Taylor number Ta_{oc} for oscillatory convection as

$$q_{oc} = \left\{\frac{1}{[2(1+Pr)]^{\frac{1}{2}}}\left(\frac{R_1-R_2}{3}\right)^{\frac{1}{2}} - \pi^2\right\}^{\frac{1}{2}}, \tag{3.29}$$

$$Ta_{oc} = (R_1-R_2)\left[\left(\frac{1+Pr}{2^3Pr^4}\right)^{\frac{1}{2}}\left(\frac{R_1-R_2}{R_{1rb}}\right)^{\frac{1}{2}} - \frac{1+Pr}{2Pr^2}\right]. \tag{3.30}$$

The coefficient

$$\left(\frac{1+Pr}{2^3Pr^4}\right)^{\frac{1}{2}}$$

of $(R_1 - R_2)$ in Eq. (3.30) is equal to unity at $Pr = Pr_c = 0.67659$ and it is less than unity for $Pr > Pr_c$. When $Pr > Pr_c$, we do not get oscillatory convection. For $Pr < Pr_c$, Eq. (3.27) intersects Eq. (3.30) at

$$R_{1ct} = R_2 + (1+\Upsilon)^2 R_{1rb}, \quad Ta_{ct} = \Upsilon(1+\Upsilon)^2 R_{1rb}, \tag{3.31}$$

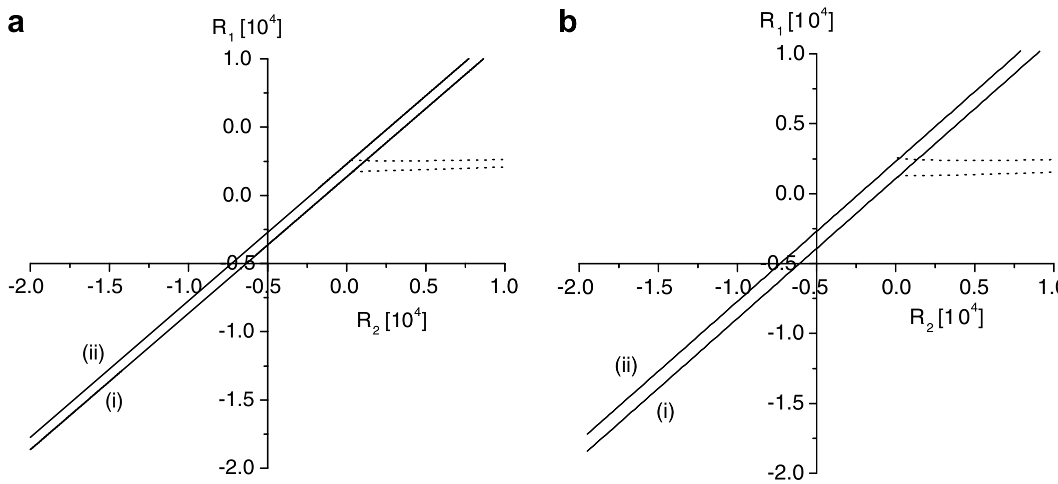

Fig. 4. Each solid line stands for stationary convection and dotted line stands for oscillatory convection. The intersection point of solid and dotted line in (a) is a Takens–Bogdanov bifurcation point and the intersection point of solid and dotted line in (b) is a co-dimension two bifurcation point. These figures are plotted for $Pr = 0.5, L = 0.1$, (i) $Ta = 300$ (ii) $Ta = 2000$.

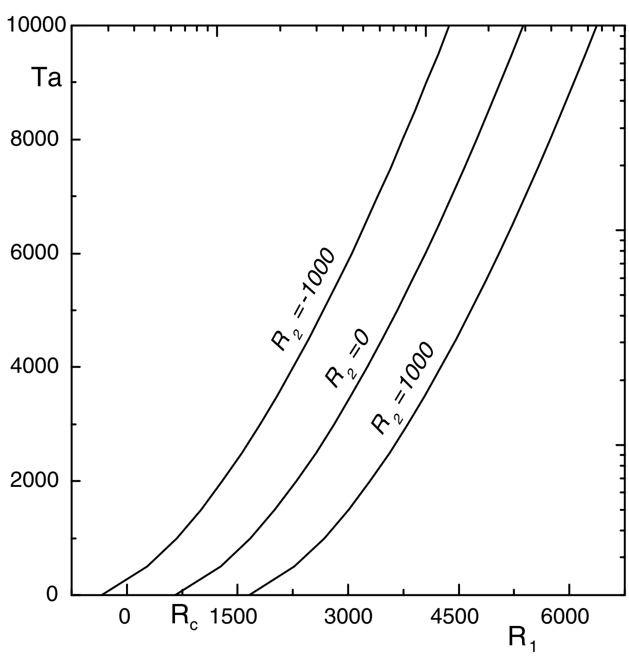

Fig. 5. The lines are plotted for $R_2 = -1000$, $R_2 = 0$ and $R_2 = 1000$. On each curve $E = 0$, on the left region of each curve $E > 0$ and on the right region of each curve $E < 0$. $E > 0$ gives stable region and $E < 0$ gives unstable region.

where

$$\Upsilon = \frac{2^{\frac{1}{2}}(1+Pr) - (1+Pr)^{\frac{1}{2}}}{(1+Pr)^{\frac{1}{2}} - 2^{\frac{3}{2}}Pr^2}.$$

In above Eq. (3.31), Ta_{ct} is also obtained by Pearlstein [6] in Appendix (A4). The suffix ct in Eq. (3.31) stands for parameter at co-dimension two bifurcation point. The thermal Rayleigh number $R_1 = R_{1ct}$ is obtained by equating Eqs. (3.27) and (3.30). Substituting $R_1 = R_{1ct}$ either into Eqs. (3.27) or (3.30), we get $Ta = Ta_{ct}$. At Ta_{ct}, $Ta_{sc} = Ta_{oc}$ and $q_{sc} \neq q_{oc}$. At $Pr = Pr_c$, $Ta_{oc} \to Ta_{sc}$ asymptotically as $R_1 \to \infty$ i.e., the intersection between Eqs. (3.27) and (3.30) appears at infinity. Figs. 8a–d show that with decreasing $Pr < Pr_c$, Ta_{ct} and R_{1ct} decreases. Thus at $Pr = 0$, we get co-dimension two bifurcation point at $R_{1ct} = 2R_{1rb} + R_2$ and $Ta_{ct} = 2(2^{\frac{1}{2}} - 1)R_{1rb}$. In Figs. 7 and 8, when $Ta < Ta_{ct}$, we get stationary convection as a first instability while for $Ta > Ta_{ct}$ the first instability will be oscillatory convection.

4. Derivation of Landau–Ginzburg equation at the onset of stationary convection

In this section the evolution of a general pattern is developed by means of a multiple scale analysis used by Newell and Whitehead [5]. A small amplitude convection cell is imposed on the basic flow. If this amplitude is of size of $O(\epsilon)$ then the interaction of the cell with itself forces a second harmonic and a mean state of correction of size $O(\epsilon^2)$ and these in turn drives an $O(\epsilon^3)$ correction to the fundamental component of the imposed roll. A solvability criterion for this last correction yields an equation of the complex valued amplitude $A(X, Y, T)$ of the imposed disturbance, the two-dimensional Landau–Ginzburg equation. To simplify the problem we assume the formation of cylindrical rolls with axis parallel to y-axis so that y-dependence disappears from Eq. (2.9). The z-dependence is contained entirely in the sin and cosine functions, which ensures that the free-free boundary conditions are satisfied. For values of the control parameter $R_1 = R_{1s}$ close to the threshold value $R_{1sc}(\epsilon^2 \ll 1)$, we assume solutions of Eqs. (2.2)–(2.5) in the power of ϵ

$$f = \epsilon f_o + \epsilon^2 f_1 + \epsilon^3 f_2 + \ldots, \tag{4.1}$$

where

$$\epsilon^2 = \frac{R_1 - R_{1sc}}{R_{1sc}} \ll 1, \tag{4.2}$$

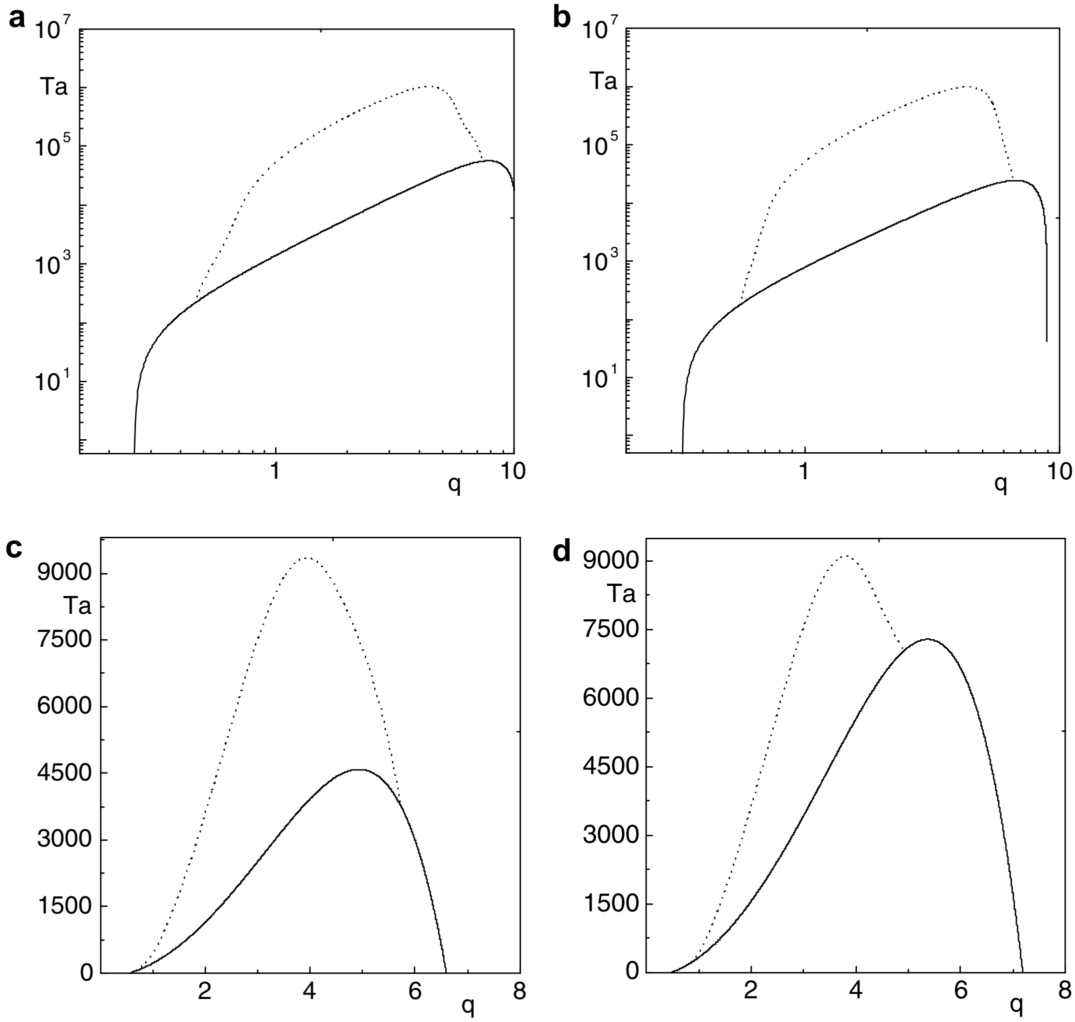

Fig. 6. On solid lines we have taken Taylor number for stationary convection and on dotted lines we have taken Taylor number for oscillatory convection. Figures are plotted for $R_1 = 5000$, (a) $L = 0.1$, $Pr = 0.05$, $R_2 = -1000$, (b) $L = 0.1$, $Pr = 0.05$, $R_2 = -400$, (c) $L = 0.2$, $Pr = 0.5$, $R_2 = 300$ and (d) $L = 0.2$, $Pr = 0.5$, $R_2 = 100$.

and $f = f(u, v, w, \theta, C)$, with the first approximation is given by the eigenvector of the linearized problem:

$$
\begin{aligned}
u_o &= \frac{\mathrm{i}\pi}{q_{\mathrm{sc}}}[A(X,Y,T)\mathrm{e}^{\mathrm{i}q_{\mathrm{sc}}x}\cos\pi z - \text{c.c.}],\\
v_o &= -\frac{\mathrm{i}\pi Ta^{\frac{1}{2}}}{\varpi_{\mathrm{sc}}^2 q_{\mathrm{sc}}}[A(X,Y,T)\mathrm{e}^{\mathrm{i}q_{\mathrm{sc}}x}\cos\pi z - \text{c.c.}],\\
w_o &= A(X,Y,T)\mathrm{e}^{\mathrm{i}q_{\mathrm{sc}}x}\sin\pi z + \text{c.c.},\\
\theta_o &= \frac{1}{\varpi_{\mathrm{sc}}^2}[A(X,Y,T)\mathrm{e}^{\mathrm{i}q_{\mathrm{sc}}x}\sin\pi z + \text{c.c.}],\\
C_o &= \frac{1}{\varpi_{\mathrm{sc}}^2 L}[A(X,Y,T)\mathrm{e}^{\mathrm{i}q_{\mathrm{sc}}x}\sin\pi z + \text{c.c.}].
\end{aligned}
\tag{4.3}
$$

Here c.c. represents the complex conjugate, $\mathrm{e}^{\mathrm{i}q_{\mathrm{sc}}x}\sin\pi z$ is the critical mode for the linear problem at $R_{1\mathrm{s}} = R_{1\mathrm{sc}}$. The complex amplitude $A(X,Y,T)$ depends on the slow variables. The independent variables x, y, z, t are scaled by introducing multiple scales

$$X = \epsilon x, \quad Y = \epsilon^{\frac{1}{2}} y, \quad z = z, \quad T = \epsilon^2 t, \tag{4.4}$$

and these formally separate the fast and slow independent variables in dependent variables u, v, w, θ, C. The differential operators can be expressed as

$$\frac{\partial}{\partial x} \to \frac{\partial}{\partial x} + \epsilon\frac{\partial}{\partial X}, \quad \frac{\partial}{\partial y} \to \epsilon^{\frac{1}{2}}\frac{\partial}{\partial Y}, \quad \frac{\partial}{\partial z} \to \frac{\partial}{\partial z}, \quad \frac{\partial}{\partial t} \to \epsilon^2\frac{\partial}{\partial T}. \tag{4.5}$$

Using the transformations (4.5), the linear and nonlinear operators of Eq. (2.9) can be written as

$$
\begin{aligned}
\mathscr{L} &= \mathscr{L}_o + \epsilon\mathscr{L}_1 + \epsilon^2\mathscr{L}_2 + \cdots,\\
\mathscr{N} &= \epsilon^2\mathscr{N}_o + \epsilon^3\mathscr{N}_1 + \cdots.
\end{aligned}
\tag{4.6}
$$

Using Eqs. (4.1) and (4.6), into Eq. (2.9), we get equating the coefficients of various powers of ϵ to zero

$$\mathscr{L}_o w_o = 0, \tag{4.7a}$$

$$\mathscr{L}_o w_1 + \mathscr{L}_1 w_o = \mathscr{N}_o, \tag{4.7b}$$

$$\mathscr{L}_o w_2 + \mathscr{L}_1 w_1 + \mathscr{L}_2 w_o = \mathscr{N}_1. \tag{4.7c}$$

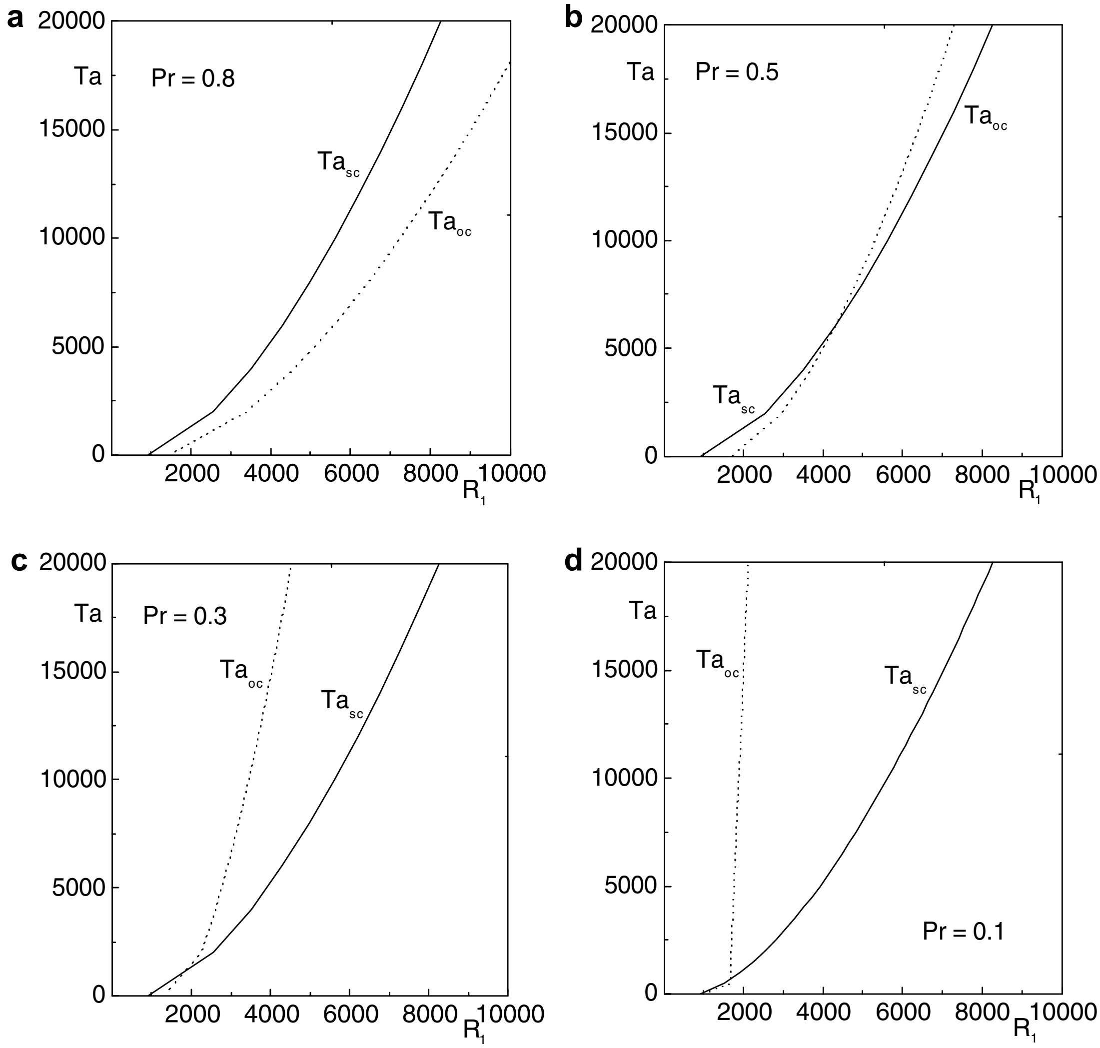

Fig. 7. In above figures solid lines are plotted for critical Taylor number Ta_{sc} (stationary convection) and dotted lines are plotted for critical Taylor number Ta_{oc} (oscillatory convection) at $R_2 = 100,\ L = 0.4$, (a) $Pr = 0.8$, (b) $Pr = 0.5$, (c) $Pr = 0.3$ and (d) $Pr = 0.1$.

Substituting the zeroth order solution w_o into $\mathscr{L}_o w_o = 0$, we get

$$q_{sc}^4(2q_{sc}^2 + 3\pi^2) - \pi^2(Ta + \pi^4) = 0. \tag{4.8}$$

Eq. (4.8) implies that q_{sc} satisfies $\left(\frac{\partial R_{1s}}{\partial q_s}\right)_{q_s = q_{sc}} = 0$. In Eq. (4.7b), $\mathscr{N}_o = 0$. $\mathscr{L}_1 w_o = 0$ and $\mathscr{N}_o = 0$ implies that Eq. (4.7b) reduces to $w_1 = 0$. Using equation of continuity we get $u_1 = 0$. Similarly $\theta_1,\ C_1,\ v_1$ are given by

$$\begin{aligned} v_1 &= \frac{-i\pi^2 Ta^{\frac{1}{2}}}{4Pr q_{sc}^3 \varpi_{sc}^2}[A^2 e^{2iq_{sc}x} - \text{c.c.}], \\ \theta_1 &= \frac{-1}{2\pi\varpi_{sc}^2}|A|^2 \sin 2\pi z, \\ C_1 &= \frac{-1}{2\pi L^2 \varpi_{sc}^2}|A|^2 \sin 2\pi z. \end{aligned} \tag{4.9}$$

Using $w_1 = 0$, Eq. (4.7c) can be written as

$$\mathscr{L}_o w_2 = \mathscr{N}_1 - \mathscr{L}_2 w_o. \tag{4.10}$$

In order that Eq. (4.10) is solvable in the presence of $\mathscr{L}_o w_o = 0$, one must require that the right-hand side of Eq. (4.10) be orthogonal to w_o which is ensured if the coefficient of $\sin \pi z$ in $\mathscr{N}_1 - \mathscr{L}_2 w_o$ is zero. This implies that

$$\lambda_o \frac{\partial A}{\partial T} - \lambda_1 \left(\frac{\partial}{\partial X} - \frac{i}{2q_{sc}} \frac{\partial^2}{\partial Y^2}\right)^2 A - \lambda_2 A + \lambda_3 |A|^2 A = 0, \tag{4.11}$$

where

$$\begin{aligned} \lambda_o &= \varpi_{sc}^2 \left\{ \left(1 + \frac{1}{L} + \frac{2}{Pr}\right)\varpi_{sc}^6 + q_{sc}^2 \left[\frac{R_2}{L}\left(1 + \frac{1}{Pr}\right) \right.\right. \\ &\qquad \left.\left. - R_{1sc}\left(\frac{1}{L} + \frac{1}{Pr}\right)\right] + Ta\pi^2\left(1 + \frac{1}{L}\right)\right\}, \\ \lambda_1 &= 4q_{sc}^2 \left[10\varpi_{sc}^6 + Ta\pi^2 + \left(\frac{R_2}{L} - R_{1sc}\right)(3q_{sc}^2 + 2\pi^2)\right], \\ \lambda_2 &= R_{1sc} q_{sc}^2 \varpi_{sc}^4, \\ \lambda_3 &= \frac{\varpi_{sc}^2 q_{sc}^2}{2}\left(R_{1sc} - \frac{R_2}{L^3}\right) - \frac{Ta\pi^4\varpi_{sc}^2}{2Pr^2 q_{sc}^2}. \end{aligned} \tag{4.12}$$

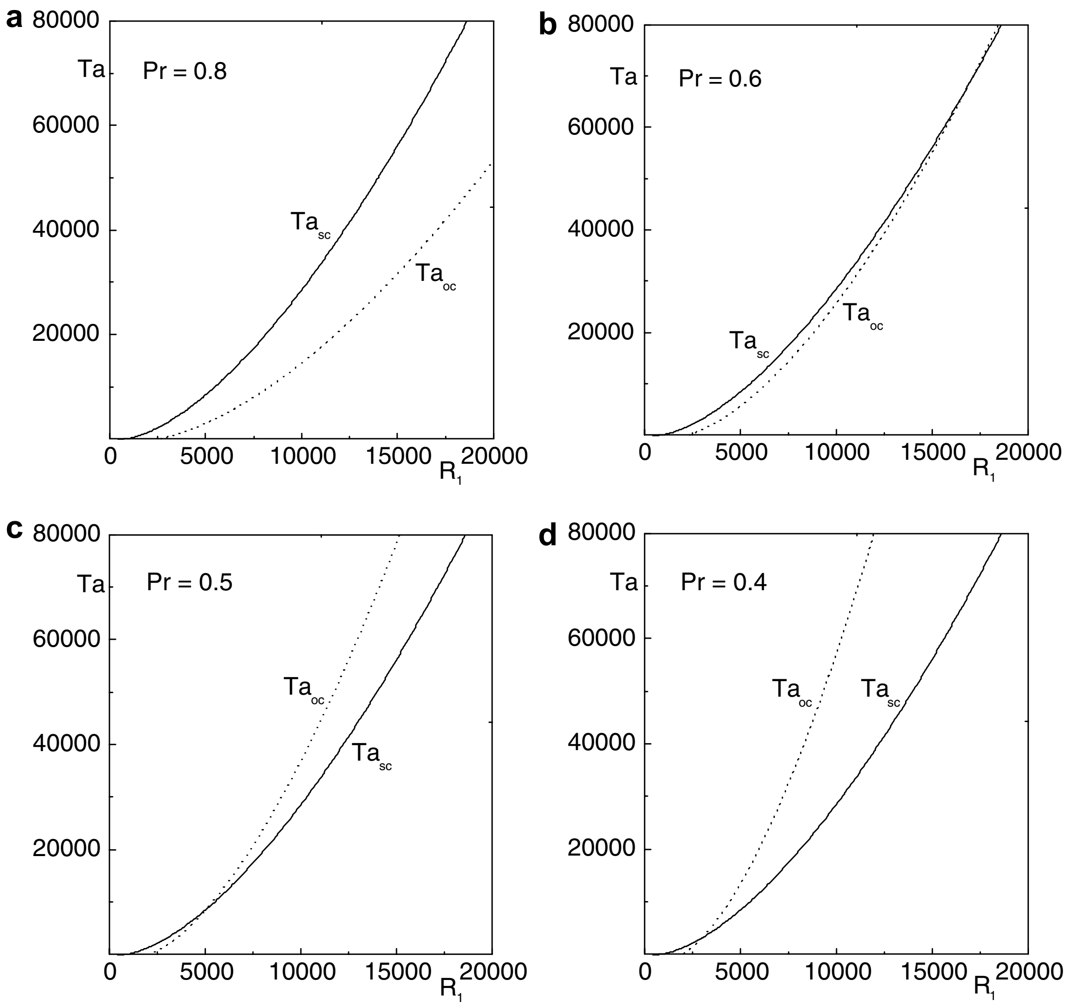

Fig. 8. The same as Fig. 7 for $L = 1$ but (a) $Pr = 0.8$, (b) $Pr = 0.6$, (c) $Pr = 0.5$, (d) $Pr = 0.4$. When $Pr \to 0$ then the intersection point appears at $R_{1ct} = (R_2/L) + R_{1rb}$ and $Ta_{ct} = 2(2^{\frac{1}{2}} - 1)R_{1rb}$, where as for $Pr \to Pr_c$, $R_{1ct} \to \infty$ and $Ta_{ct} \to \infty$.

By using the scaling (4.4) and $A(x, y, t) = A(X, Y, T)/\epsilon$, Eq. (4.11) can be written in fast variables as

$$\lambda_o \frac{\partial A}{\partial t} - \lambda_1 \left(\frac{\partial}{\partial x} - \frac{\mathrm{i}}{2q_{sc}} \frac{\partial^2}{\partial y^2} \right)^2 A - \epsilon^2 \lambda_2 A + \lambda_3 |A|^2 A = 0. \tag{4.13}$$

Equation (4.13) is a nonlinear two-dimensional time dependent Landau–Ginburg equation and describes the variation of the slow time scale $\epsilon^2 t$ and slow spatial scale ϵx perpendicular to the rolls. For $\lambda_o = 0$, we get $R_2 = R_{2c}$ [which is obtained in Eq. (3.11) with $q = q_{sc}$] and we do not get Landau–Ginzburg equation. λ_o is positive when $R_2 < R_{2c}$ and is negative when $R_2 > R_{2c}$. Substituting Ta from Eq. (3.5) and R_{1sc} from Eq. (3.6) into λ_1, we get $\lambda_1 = 12\varpi_{sc}^6 q_{sc}^2$, hence λ_1 is positive and is independent of R_2, L. The ratios λ_o/λ_2 and λ_1/λ_2 are known as growth rate amplitude and the curvature of the marginal stability curve, respectively. They are defined as

$$\frac{\lambda_o}{\lambda_2} = \left(R_{1sc} \frac{\partial p}{\partial R_1} \right)^{-1} \quad \text{and} \quad \frac{\lambda_1}{\lambda_2} = \frac{1}{2R_{1sc}} \frac{\partial^2 R_{1s}}{\partial q_s^2} \quad \text{at } q_s = q_{sc}.$$

The parameters λ_o/λ_2 and λ_1/λ_2 decrease as $R_2 \to R_{2c}$, when $R_2 < R_{2c}$. Here λ_2 always positive. For $\lambda_3 > 0$, we get forward bifurcation (supercritical pitchfork bifurcation) and for $\lambda_3 < 0$ we get backward bifurcation. Landau–Ginzburg equation is valid only for $\lambda_3 > 0$. At $\lambda_3 = 0$, we get tricritical bifurcation point (see Fig. 9). From this figure it is clear that large Taylor number required to get $\lambda_3 > 0$ and an inverse relation exist between Ta, Pr to get $\lambda_3 > 0$.

Dropping the t-dependence and y-dependence terms from Eq. (4.13), we get

$$\frac{\mathrm{d}^2 A}{\mathrm{d}x^2} + \frac{\epsilon^2 \lambda_2}{\lambda_1} \left(1 - \frac{\lambda_3}{\epsilon^2 \lambda_2} |A|^2 \right) A = 0. \tag{4.14}$$

Solution of Eq. (4.14) is given by

$$A(x) = A_o \tanh\left(\frac{x}{\Lambda} \right), \tag{4.15}$$

where

$$A_o = \left(\frac{\epsilon^2 \lambda_2}{\lambda_3} \right)^{\frac{1}{2}} \quad \text{and} \quad \Lambda = \left(\frac{2\lambda_1}{\epsilon^2 \lambda_2} \right)^{\frac{1}{2}}.$$

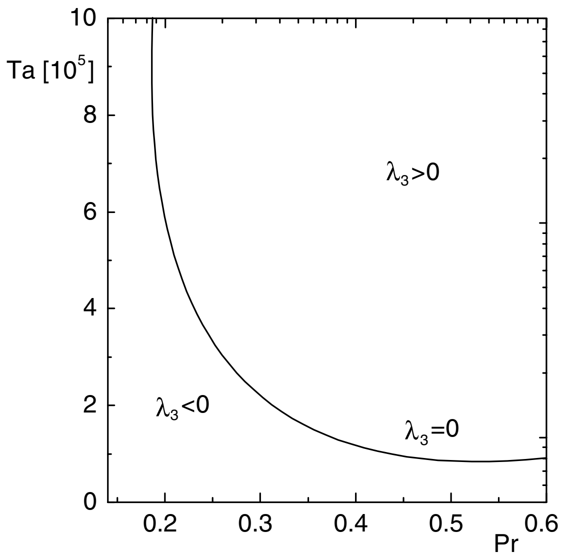

Fig. 9. λ_3 is the coefficient of nonlinear term of Landau–Ginzburg equation (4.11), which explains the type of pitchfork bifurcation. The bifurcation is supercritical if $\lambda_3 > 0$ and subcritical if $\lambda_3 < 0$. $\lambda_3 = 0$ gives tricritical bifurcation point.

4.1. Long wave-length instabilities

In order to study the properties of a structure with a given phase winding number $\delta q_s = q - q_{sc}$, we substitute

$$A(x,y,t) = A_1(x,y,t)e^{i\delta q_s x} \quad \text{(stationary solutions)}, \tag{4.16}$$

into Eq. (4.13) and we obtain

$$\lambda_o \frac{\partial A_1}{\partial t} = (\epsilon^2\lambda_2 - \lambda_1\delta q_s^2)A_1 + 2i\lambda_1\delta q_s\left(\frac{\partial}{\partial x} - \frac{i}{2q_{sc}}\frac{\partial^2}{\partial y^2}\right)A_1 + \lambda_1\left(\frac{\partial}{\partial x} - \frac{i}{2q_{sc}}\frac{\partial^2}{\partial y^2}\right)^2 A_1 - \lambda_3|A_1|^2A_1 = 0. \tag{4.17}$$

The steady state uniform solution of Eq. (4.17) is

$$A_1 = A_{1o} = \left[\frac{(\epsilon^2\lambda_2 - \lambda_1\delta q_s^2)}{\lambda_3}\right]^{\frac{1}{2}}. \tag{4.18}$$

Let $\tilde{u}(x,y,t) + i\tilde{v}(x,y,t)$ be an infinitesimal perturbation from a uniform steady state solution A_{1o} given by Eq. (4.18). Now substituting

$$A_1 = \left[\frac{(\epsilon^2\lambda_2 - \lambda_1\delta q_s^2)}{\lambda_3}\right]^{\frac{1}{2}} + \tilde{u} + i\tilde{v}$$

into Eq. (4.17) and equating real and imaginary parts, we obtain

$$\lambda_o \frac{\partial \tilde{u}}{\partial t} = \left[-2(\epsilon^2\lambda_2 - \lambda_1\delta q_s^2) + \lambda_1\frac{\partial^2}{\partial x^2} + \frac{\lambda_1\delta q_s}{q_{sc}}\frac{\partial^2}{\partial y^2} - \frac{\lambda_1}{4q_{sc}^2}\frac{\partial^4}{\partial y^4}\right]\tilde{u} - \left(2\lambda_1\delta q_s - \frac{\lambda_1}{q_{sc}}\frac{\partial^2}{\partial y^2}\right)\frac{\partial \tilde{v}}{\partial x}, \tag{4.19a}$$

$$\lambda_o \frac{\partial \tilde{v}}{\partial t} = \left(2\lambda_1\delta q_s - \frac{\lambda_1}{q_{sc}}\frac{\partial^2}{\partial y^2}\right)\frac{\partial \tilde{u}}{\partial x} + \lambda_1\left(\frac{\partial^2}{\partial x^2} + \frac{\delta q_s}{q_{sc}}\frac{\partial^2}{\partial y^2} - \frac{1}{4q_{sc}^2}\frac{\partial^4}{\partial y^4}\right)\tilde{v}. \tag{4.19b}$$

We analyze Eqs. (4.19a) and (4.19b) by using normal modes of the form

$$\tilde{u} = Ue^{(St)}\cos(q_x x)\cos(q_y y),$$
$$\tilde{v} = Ve^{(St)}\sin(q_x x)\cos(q_y y). \tag{4.20}$$

Putting solutions (4.20) into Eqs. (4.19a) and (4.19b) we get,

$$\left[\lambda_o S + 2(\epsilon^2\lambda_2 - \lambda_1\delta q_s^2) + \lambda_1 q_x^2 + \frac{\lambda_1\delta q_s}{q_{sc}}q_y^2 + \frac{\lambda_1}{4q_{sc}^2}q_y^4\right]U + \left(2\delta q_s + \frac{q_y^2}{q_{sc}}\right)\lambda_1 q_x V = 0, \tag{4.21a}$$

$$\lambda_1 q_x\left(2\delta q_s + \frac{q_y^2}{q_{sc}}\right)U + \left(\lambda_o S + \lambda_1 q_x^2 + \frac{\lambda_1\delta q_s}{q_{sc}}q_y^2 + \frac{\lambda_1}{4q_{sc}^2}q_y^4\right)V = 0. \tag{4.21b}$$

On solving Eqs. (4.21a) and (4.21b) we get,

$$\lambda_o^2S^2 + 2S\left[2\lambda_o(\epsilon^2\lambda_2 - \lambda_1\delta q_s^2) + \lambda_o\lambda_1 q_x^2 + \frac{\lambda_o\lambda_1}{q_{sc}}q_y^2\delta q_s + \frac{\lambda_o\lambda_1}{4q_{sc}^2}q_y^4\right] + \left[2(\epsilon^2\lambda_2 - \lambda_1\delta q_s^2) + \lambda_1 q_x^2 + \frac{\lambda_1}{q_{sc}}q_y^2\delta q_s + \frac{\lambda_1}{4q_{sc}^2}q_y^4\right] \times \left[\lambda_1 q_x^2 + \frac{\lambda_1\delta q_s}{q_{sc}}q_y^2 + \frac{\lambda_1}{4q_{sc}^2}q_y^4\right] - q_x^2\left(2\lambda_1\delta q_s + \frac{\lambda_1}{q_{sc}}q_y^2\right)^2 = 0, \tag{4.22}$$

whose roots ($S\pm$) are real. Here ($S\pm$) defined as

$$S(\pm) = -\frac{1}{\lambda_o^2}\left\{\left[2\lambda_o(\epsilon^2\lambda_2 - \lambda_1\delta q_s^2) + \lambda_o\lambda_1 q_x^2 + \frac{\lambda_o\lambda_1}{q_{sc}}q_y^2\delta q_s + \frac{\lambda_o\lambda_1}{4q_{sc}^2}q_y^4\right] \pm \left[(2\lambda_o(\epsilon^2\lambda_2 - \lambda_1\delta q_s^2))^2 + \lambda_1^2 q_x^2\left(2\delta q_s + \frac{q_y^2}{q_{sc}}\right)^2\right]^{\frac{1}{2}}\right\}, \tag{4.23}$$

solution $S(-)$ is clearly negative, thus the corresponding mode is stable and if $S(+)$ is positive then rolls can be unstable. Symmetry considerations help us to restrict the study of S(+) to a domain ($q_x \geqslant 0,\ q_y \geqslant 0$).

4.1.1. Longitudinal perturbations and Eckhaus instability

Inserting $q_y = 0$ into (4.22), we get

$$\lambda_o^2S^2 + 2S(2\lambda_o(\epsilon^2\lambda_2 - \lambda_1\delta q_s^2) + \lambda_o\lambda_1 q_x^2) + \lambda_1 q_x^2[2(\epsilon^2\lambda_2 - 3\lambda_1\delta q_s^2) + q_x^2] = 0.$$

Since the roots are real and their sum is always negative, the pattern is stable as long as both roots are negative, i.e., their product is positive. The cell pattern becomes unstable when the product is negative, i.e., when

$$q_x^2 \geqslant 2\left(\delta q_s^2 - \frac{\lambda_2}{\lambda_1}\right) \quad \text{and} \quad q_x^2 \leqslant 2(3\lambda_1\delta q_s^2 - \epsilon^2\lambda_2),$$

for this requires $\sqrt{\frac{\epsilon^2\lambda_2}{3\lambda_1}} \leqslant |\delta q_s| \leqslant \sqrt{\frac{\epsilon^2\lambda_2}{\lambda_1}}$; this condition defines the domain of the Eckhaus instability. The above condition implies that the most unstable wave vector tends to zero, when $|\delta q_s| \to \sqrt{\frac{\epsilon^2\lambda_2}{3\lambda_1}}$.

4.1.2. Transverse perturbations and zigzag instability

Let us consider $q_x = 0$ into (4.22), we get

$$\lambda_o^2S^2 + 2S\left[2\lambda_o(\epsilon^2\lambda_2 - \lambda_1\delta q_s^2) + \frac{\lambda_o\lambda_1}{q_{sc}}q_y^2\delta q_s + \frac{\lambda_o\lambda_1}{4q_{sc}^2}q_y^4\right] + \left[2(\epsilon^2\lambda_2 - \lambda_1\delta q_s^2) + \frac{\lambda_1}{q_{sc}}q_y^2\delta q_s + \frac{\lambda_1}{4q_{sc}^2}q_y^4\right] \times \left[\frac{\delta q_s}{q_{sc}} + \frac{q_y^2}{4q_{sc}^2}\right]\lambda_1 q_y^2 = 0.$$

The two eigen modes are uncoupled and we have $S(-)$,

$$S(-) = -2(\epsilon^2\lambda_2 - \lambda_1\delta q_s^2) - \frac{\lambda_1}{q_{sc}}q_y^2\delta q_s - \frac{\lambda_1}{4q_{sc}^2}q_y^4 < 0,$$

for one of them. The other is amplified when

$$S(+) = -\lambda_1 q_y^2\left(\delta q_s + \frac{q_y^2}{4q_{sc}}\right) > 0.$$

This implies that $\delta q_s < 0$ defines the domain of the zigzag instability. Since $\lambda_1 > 0$, we get $|\delta q_s| > q_y^2/4q_{sc}$.

We have studied the effect of rotation rate on long wave length instabilities and observed that the Eckhuas instability and zigzag instability regions increases when Ta increases (see Fig. 10). In this figure we can see that $\delta q_s \to 0$ as $q \to q_{sc}$. This result is true for other parameters also.

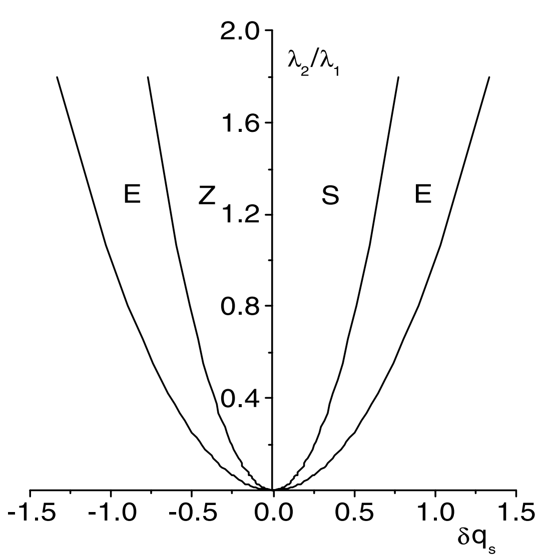

Fig. 10. Regions of Eckhuas instability (E), zigzag instability (Z) and stable region (S) are plotted for $L = 0.1$, $Pr = 0.5$ and $R_2 = 1000$.

4.2. Heat transport by convection

The maximum of steady amplitude A is denoted by $|A_{max}|$ which is given as

$$|A_{max}| = \left(\frac{\epsilon^2\lambda_2}{\lambda_3}\right)^{\frac{1}{2}}. \tag{4.24}$$

Equation (4.24) is obtained either from Eq. (4.15) with $\tanh(x/\Lambda) = 1$ or from Eq. (4.16), with $\delta q_s = 0$ and $A_1 = A_{1o}$. We use $|A_{max}|$ to calculate Nusselt number Nu. To discuss the heat transfer near the neutral region, we express it through the Nusselt number. The Nusselt number defined as

$$Nu = \frac{Hd}{\kappa\Delta T'}$$

which is the ratio of the heat transported across any layer to the heat which would be transported by conduction alone. Here H is the rate of heat transfer per unit area and is defined as

$$H = -\left\langle\frac{\partial T_{total}}{\partial z'}\right\rangle_{z'=0}, \tag{4.25}$$

where $T_{total} = \theta' + T_b' - z'\Delta T'$. In (4.25), angular brackets correspond to a horizontal average. The Nusselt number can be calculated in terms of amplitude A and it is given as

$$Nu = 1 + \frac{\epsilon^2}{\varpi_{sc}^2}|A_{max}|^2. \tag{4.26}$$

From Eq. (4.26), we get conduction for $R_1 \leqslant R_{1sc}$ and convection for $R_1 > R_{1sc}$.

Since the amplitude equation is valid for $\lambda_3 > 0$, this is possible for $R_1 > R_{1sc}$ (supercritical). We observed that for $R_2 > 0$, large Taylor number is required to get $\lambda_3 > 0$. Thus we get $Nu > 1$ for $R_1 > R_{1sc}$. We get convection for $Nu > 1$ and conduction for $Nu = 1$. For the case of stationary convection as Nusselt number Nu increases heat conducted by steady mode increases.

In the problem of double diffusive convection with rotation, Nu depends on R_2, Pr, Ta and L. We have computed Nu for different values of Ta, for some fixed values of other parameters and observed that Nu increases as Ta decreases (see Fig. 11). This implies that rotation rate inhibits the heat transport. Similar result obtained for L, that is when L increases Nu decreases. In non rotating convective problems λ_3 does not depend on Pr. But for rotating problems λ_3 always depends on Pr. The Nusselt number shows two different results depending on Pr. That is for $Pr \leqslant Pr_c$, as Pr increases then Nu increases. For $Pr > Pr_c$, when Pr increases then Nu decreases. Finally we have studied the effect of R_2 on Nu, and found that Nu increases as R_2 increases.

5. Derivation of Landau–Ginzburg type equations at the onset of oscillatory convection

To derive coupled Landau–Ginzburg type equations we consider the following scaling.

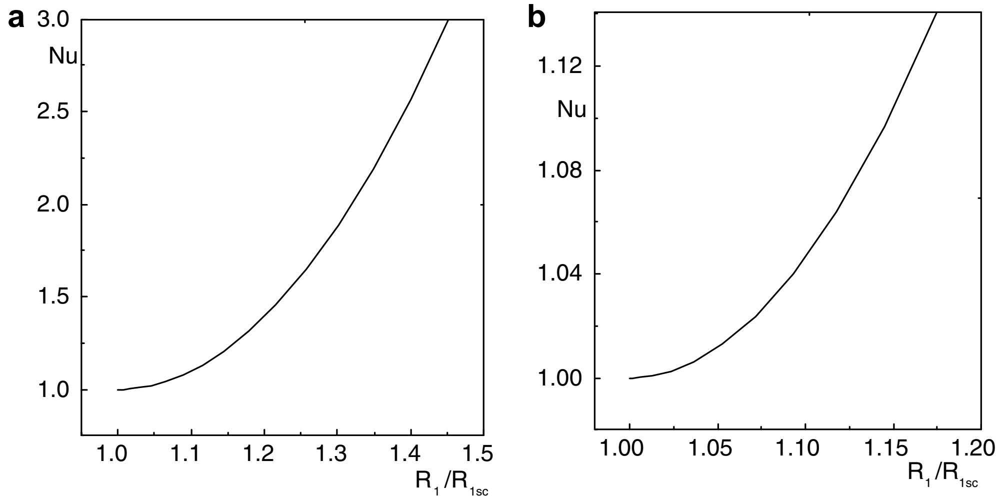

Fig. 11. (a) is plotted for $Ta = 10^5$ and (b) is plotted for $Ta = 2\times10^5$ for the fixed values of $L = 0.1,\ R_2 = 10,\ Pr = 0.5$. In both figures solid lines start from $Nu = 1$.

$$X = \epsilon x, \quad \tau = \epsilon t, \quad T = \epsilon^2 t, \tag{5.1}$$

where $\epsilon^2 = R_1/R_{1oc} - 1 \ll 1$ and R_{1oc} is a critical thermal Rayleigh number of oscillatory convection.

From (5.1) the differential operators $\partial/\partial x, \partial/\partial t$ can be written as

$$\frac{\partial}{\partial x} \to \frac{\partial}{\partial x} + \epsilon\frac{\partial}{\partial X}, \quad \frac{\partial}{\partial t} \to \frac{\partial}{\partial t} + \epsilon\frac{\partial}{\partial \tau} + \epsilon^2\frac{\partial}{\partial T}. \tag{5.2}$$

We write the solutions of Eqs. (2.2)–(2.5) in the power series of ϵ given as follows

$$f = \epsilon f_o + \epsilon^2 f_1 + \epsilon^3 f_2 + \cdots \tag{5.3}$$

where $f = f(u, v, w, \omega_x, \omega_y, \omega_z, \theta, C)$, with the first approximation is given by

$$\begin{aligned}
u_o &= \frac{\pi \mathrm{i}}{q_{oc}}[A_{1L}e^{\mathrm{i}(\omega_{oc}t+q_{oc}x)} - A_{1R}e^{\mathrm{i}(\omega_{oc}t-q_{oc}x)} - \text{c.c.}]\cos\pi z,\\
v_o &= \frac{-Ta^{\frac12}\pi\mathrm{i}}{q_{oc}}\left[\frac{A_{1L}e^{\mathrm{i}(\omega_{oc}t+q_{oc}x)} - A_{1R}e^{\mathrm{i}(\omega_{oc}t-q_{oc}x)}}{\left(\varpi_{oc}^2 + \frac{\mathrm{i}\omega_{oc}}{Pr}\right)} - \text{c.c.}\right]\cos\pi z,\\
w_o &= [A_{1L}e^{\mathrm{i}(\omega_{oc}t+q_{oc}x)} + A_{1R}e^{\mathrm{i}(\omega_{oc}t-q_{oc}x)} + \text{c.c.}]\sin\pi z,\\
C_o &= \frac{1}{L}\left[\frac{A_{1L}e^{\mathrm{i}(\omega_{oc}t+q_{oc}x)} + A_{1R}e^{\mathrm{i}(\omega_{oc}t-q_{oc}x)}}{\left(\varpi_{oc}^2 + \frac{\mathrm{i}\omega_{oc}}{L}\right)} + \text{c.c.}\right]\sin\pi z,\\
\theta_o &= \left[\frac{A_{1L}e^{\mathrm{i}(\omega_{oc}t+q_{oc}x)} + A_{1R}e^{\mathrm{i}(\omega_{oc}t-q_{oc}x)}}{(\varpi_{oc}^2 + \mathrm{i}\omega_{oc})} + \text{c.c.}\right]\sin\pi z,
\end{aligned} \tag{5.4}$$

where $\varpi_{oc}^2 = q_{oc}^2 + \pi^2$, c.c. stands for complex conjugate and A_{1L} and A_{1R} are slow varying amplitude functions of left and right travelling waves.

By substituting the definitions of (5.2) and (5.3) into Eq. (2.9) and equating the coefficients of ϵ, ϵ^2, ϵ^3 to zero, we get

$$\mathscr{L}_o w_o = 0, \tag{5.5a}$$
$$\mathscr{L}_1 w_o + \mathscr{L}_o w_1 = \mathscr{N}_o, \tag{5.5b}$$
$$\mathscr{L}_2 w_o + \mathscr{L}_1 w_1 + \mathscr{L}_o w_2 = \mathscr{N}_1. \tag{5.5c}$$

From linear equation (5.5a), we get critical Rayleigh number. At $O(\epsilon^2)$, $\mathscr{N}_o = 0$ and $\mathscr{L}_1 w_o = 0$ gives

$$\frac{\partial A_{1L}}{\partial \tau} - v_g\frac{\partial A_{1L}}{\partial X} = 0 \quad \text{and} \quad \frac{\partial A_{1R}}{\partial \tau} + v_g\frac{\partial A_{1R}}{\partial X} = 0, \tag{5.6}$$

where $v_g = \left(\frac{\partial\omega}{\partial q}\right)_{q=q_{oc}}$ is the group velocity and is real. Hence we get $w_1 = 0$. Using this fist order solution, from equation of continuity we get $u_1 = 0$. The remaining first order solutions v_1, θ_1 and C_1 are obtained from the following equations:

$$\left(\frac{1}{Pr}\frac{\partial}{\partial t} - \nabla^2\right)\frac{\partial v_1}{\partial x} = Ta^{\frac12}\frac{\partial w_1}{\partial z} - \frac{1}{Pr}[(\vec{V}_o\cdot\nabla)\omega_{z_o} - (\vec{\omega}_o\cdot\nabla)w_o], \tag{5.7a}$$

$$\left(\frac{\partial}{\partial t} - \nabla^2\right)\theta_1 = w_1 - (\vec{V}_o\cdot\nabla)\theta_o, \tag{5.7b}$$

$$\left(\frac{1}{L}\frac{\partial}{\partial t} - \nabla^2\right)C_1 = \frac{w_1}{L} - \frac{1}{L}(\vec{V}_o\cdot\nabla)C_o. \tag{5.7c}$$

By using zeroth order solutions into Eqs. (5.7a)–(5.7c) we get

$$\begin{aligned}
v_1 &= \frac{-\mathrm{i}Ta^{\frac12}\pi^2}{2Prq_{oc}}\left[\frac{A_{1L}^2e^{2\mathrm{i}(\omega_{oc}t+q_{oc}x)}}{\left(2q_{oc}^2+\frac{\mathrm{i}\omega_{oc}}{Pr}\right)\left(\varpi_{oc}^2+\frac{\mathrm{i}\omega_{oc}}{Pr}\right)}\right.\\
&\quad\left.-\frac{A_{1R}^2e^{2\mathrm{i}(\omega_{oc}t-q_{oc}x)}}{\left(2q_{oc}^2+\frac{\mathrm{i}\omega_{oc}}{Pr}\right)\left(\varpi_{oc}^2+\frac{\mathrm{i}\omega_{oc}}{Pr}\right)} + \frac{\varpi_{oc}^2e^{2\mathrm{i}q_{oc}x}A_{1L}A_{1R}^*}{q_{oc}^2\left(\varpi_{oc}^4+\frac{\omega_{oc}^2}{Pr^2}\right)} - \text{c.c.}\right],\\
C_1 &= \frac{-\pi}{L^2}\left[\frac{\varpi_{oc}^2(|A_{1L}|^2+|A_{1R}|^2)}{2\pi^2\left(\varpi_{oc}^2+\frac{\omega_{oc}^2}{L^2}\right)} + \frac{A_{1L}A_{1R}e^{2\mathrm{i}\omega_{oc}t}}{\left(2\pi^2+\frac{\mathrm{i}\omega_{oc}}{L}\right)\left(\varpi_{oc}^2+\frac{\mathrm{i}\omega_{oc}}{L}\right)} + \text{c.c.}\right]\sin 2\pi z,\\
\theta_1 &= -\pi\left[\frac{(|A_{1L}|^2+|A_{1R}|^2)\varpi_{oc}^2}{2\pi^2(\varpi_{oc}^4+\omega_{oc}^2)} + \frac{A_{1L}A_{1R}e^{2\mathrm{i}\omega_{oc}t}}{(2\pi^2+\mathrm{i}\omega_{oc})(\varpi_{oc}^2+\mathrm{i}\omega_{oc})} + \text{c.c.}\right]\sin 2\pi z.
\end{aligned} \tag{5.8}$$

The solvability criterion of Eq. (5.5c) gives the following coupled amplitude equations, known as Landau–Ginzburg type equations

$$\Lambda_o \frac{\partial A_{1L}}{\partial T} + \Lambda_1\left(\frac{\partial}{\partial \tau} - v_g\frac{\partial}{\partial X}\right)A_{2L} - \Lambda_2\frac{\partial^2 A_{1L}}{\partial X^2} - \Lambda_3 A_{1L} + \Lambda_4|A_{1L}|^2 A_{1L} + \Lambda_5|A_{1R}|^2 A_{1L} = 0, \tag{5.9a}$$

$$\Lambda_o \frac{\partial A_{1R}}{\partial T} + \Lambda_1\left(\frac{\partial}{\partial \tau} + v_g\frac{\partial}{\partial X}\right)A_{2R} - \Lambda_2\frac{\partial^2 A_{1R}}{\partial X^2} - \Lambda_3 A_{1R} + \Lambda_4|A_{1R}|^2 A_{1R} + \Lambda_5|A_{1L}|^2 A_{1R} = 0, \tag{5.9b}$$

where Λ_o, Λ_1, Λ_2, Λ_3, Λ_4 and Λ_5 are the complex coefficients in physical parameters q_{oc}, R_{1oc}, R_2, L and Ta. Here

$$A_{2L} = \left(\frac{\partial}{\partial \tau} + v_g\frac{\partial}{\partial X}\right)A_{1L} \quad \text{and} \quad A_{2R} = \left(\frac{\partial}{\partial \tau} - v_g\frac{\partial}{\partial X}\right)A_{1R}.$$

Clearly A_{1L}, A_{1R} are of order ϵ and A_{2L}, A_{2R} are of order ϵ^2. From Eqs. (5.6), we get $A_{1L}(\xi', T)$ and $A_{1R}(\eta', T)$, where $\xi' = v_g\tau + X$, $\eta' = v_g\tau - X$. Equations (5.9a), (5.9b) can be written as

$$2v_g\Lambda_1\frac{\partial A_{2L}}{\partial \eta'} = -\Lambda_o\frac{\partial A_{1L}}{\partial T} + \Lambda_2\frac{\partial^2 A_{1L}}{\partial X^2} + \Lambda_3 A_{1L} - \left(\Lambda_4|A_{1L}|^2 + \Lambda_5|A_{1R}|^2\right)A_{1L}, \tag{5.10a}$$

$$2v_g\Lambda_1\frac{\partial A_{2R}}{\partial \xi'} = -\Lambda_o\frac{\partial A_{1R}}{\partial T} + \Lambda_2\frac{\partial^2 A_{1R}}{\partial X^2} + \Lambda_3 A_{1R} - (\Lambda_4|A_{1R}|^2 + \Lambda_5|A_{1L}|^2)A_{1R}. \tag{5.10b}$$

Let $\xi'\epsilon[0, l_1]$, $\eta'\epsilon[0, l_2]$, where l_1, l_2 are periods of A_{1L}, A_{1R}, respectively. Expansion (5.3) remains asymptotic for times $t = O(\epsilon^{-2})$ only if an appropriate solvability condition holds. This condition obtained by integrating Eq. (5.10a) over η' and Eq. (5.10b) over ξ', we get

$$\Lambda_o\frac{\partial A_{1L}}{\partial T} = \Lambda_2\frac{\partial^2 A_{1L}}{\partial X^2} + \Lambda_3 A_{1L} - (\Lambda_4|A_{1L}|^2 + \Lambda_5|A_{1R}|^2)A_{1L}, \tag{5.11a}$$

$$\Lambda_o\frac{\partial A_{1R}}{\partial T} = \Lambda_2\frac{\partial^2 A_{1R}}{\partial X^2} + \Lambda_3 A_{1R} - (\Lambda_4|A_{1R}|^2 + \Lambda_5|A_{1L}|^2)A_{1R}. \tag{5.11b}$$

Equation (5.11a) is for the amplitude of left moving waves and Eq. (5.11b) is for the amplitude of right moving waves. Equations (5.11) are known as one-dimensional coupled Landau–Ginzburg equations with original slow spatial coordinate and time. These Eqs. (5.11) are correct asymptotic evolution equations when $v_g = O(1)$.

5.1. Travelling wave and standing wave convection

To study the stability regions of travelling waves and standing waves we proceed as follows:

On dropping slow space variable X from Eqs. (5.11a) and (5.11b), we get a pair of first order ordinary differential equations

$$\frac{dA_{1L}}{dT} = \beta A_{1L} + \gamma A_{1L}|A_{1L}|^2 + \delta A_{1L}|A_{1R}|^2, \tag{5.12}$$

$$\frac{dA_{1R}}{dT} = \beta A_{1R} + \gamma A_{1R}|A_{1R}|^2 + \delta A_{1R}|A_{1L}|^2, \tag{5.13}$$

where

$$\beta = \frac{\Lambda_3}{\Lambda_o}, \quad \gamma = -\frac{\Lambda_4}{\Lambda_o} \quad \text{and} \quad \delta = -\frac{\Lambda_5}{\Lambda_o}.$$

Consider $A_{1L} = a_L e^{i\phi_L}$ and $A_{1R} = a_R e^{i\phi_R}$ (we can write a complex number in the amplitude and phase (angle) form), where $a_L = |A_{1L}|$, $\phi_L = \arg(A_{1L}) = \tan^{-1}(\frac{\mathrm{Im}(A_{1L})}{\mathrm{Re}(A_{1L})})$ and $a_R = |A_{1R}|$, $\phi_R = \arg(A_{1R}) = \tan^{-1}(\frac{\mathrm{Im}(A_{1R})}{\mathrm{Re}(A_{1R})})$. a_L, a_R, ϕ_L, ϕ_R are functions of time T since A_{1L} and A_{1R} are functions of T. Thus a_L and a_R are positive functions.

Substituting the definitions of A_{1L} and A_{1R} and $\beta = \beta_1 + i\beta_2$, $\gamma = \gamma_1 + i\gamma_2$, $\delta = \delta_1 + i\delta_2$ into equations (5.12) and (5.13), we get

$$\frac{da_L}{dT} = \beta_1 a_L + \gamma_1 a_L|a_L|^2 + \delta_1 a_L|a_R|^2, \tag{5.14}$$

$$\frac{d\phi_L}{dT} = \beta_2 + \gamma_2|a_L|^2 + \delta_2|a_R|^2, \tag{5.15}$$

$$\frac{da_R}{dT} = \beta_1 a_R + \gamma_1 a_R|a_R|^2 + \delta_1 a_R|a_L|^2, \tag{5.16}$$

$$\frac{d\phi_R}{dT} = \beta_2 + \gamma_2|a_R|^2 + \delta_2|a_L|^2. \tag{5.17}$$

Eqs. (5.14) and (5.16) not contain phase term, so we take these two equations for the future discussions. We have equations (5.14) and (5.16) as

$$\frac{da_L}{dT} = \beta_1 a_L + \gamma_1 a_L^3 + \delta_1 a_L a_R^2, \tag{5.18}$$

$$\frac{da_R}{dT} = \beta_1 a_R + \gamma_1 a_R^3 + \delta_1 a_R a_L^2, \tag{5.19}$$

since a_L and a_R are positive functions. Eqs. (5.18) and (5.19) are known as coupled Landau equations. Put

$$\frac{da_L}{dT} = F_1(a_L, a_R), \quad \frac{da_R}{dT} = F_2(a_L, a_R) \tag{5.20}$$

Now we discuss the stability of equilibrium points of above equations (5.20). We get four equilibrium points like $(a_L, a_R) = (0, 0)$ [conduction state], $(a_L, a_R) = (a_L, 0)$ [a_L = amplitude of left travelling waves, here we get $F_2 = 0$, and we get one condition from $F_1 = 0$, i.e., $a_L^2 = -\frac{\beta_1}{\gamma_1}(= |A_{1L}|^2)$], $(a_L, a_R) = (0, a_R)$ [a_R = amplitude of right travelling waves, here $F_1 = 0$ and from $F_2 = 0$, we get $a_R^2 = -\frac{\beta_1}{\gamma_1}(= |A_{1R}|^2)$], and for $a_L \neq 0$ and $a_R \neq 0$ we get $(a_L, a_R) = (-\frac{\beta_1}{(\gamma_1+\delta_1)}, -\frac{\beta_1}{(\gamma_1+\delta_1)})$ [this gives condition for standing waves. At standing waves we have $A_{1L} = A_{1R}$, so $a_L = a_R$].

Now the Jacobian of F_1 and F_2 is given by

$$\begin{pmatrix} \frac{\partial F_1}{\partial a_L} & \frac{\partial F_1}{\partial a_R} \\ \frac{\partial F_2}{\partial a_L} & \frac{\partial F_2}{\partial a_R} \end{pmatrix}.$$

If real parts of all eigenvalues of the Jacobian are negative at an equilibrium point, then that point is a stable equilibrium [Lyapounov's theorem or principle of linearized stability]. Some valuable conditions for travelling waves and standing waves are: Travelling waves are stable if $\beta_1 > 0,\ \gamma_1 < 0$ and $\delta_1 < \gamma_1 < 0$. Standing waves are stable if $\beta_1 > 0, \gamma_1 < 0$ and (i) if $\delta_1 > 0$, then $-\gamma_1 > \delta_1 > 0$, (ii) if $\delta_1 < 0$, then $-\gamma_1 > -\delta_1 > 0$. At the end of this section, we have obtained exact analytical solutions of coupled Landau equations for the case of $\delta_1 = \gamma_1$ for both travelling waves and standing waves. Similar discussions can be done for the case $\delta_1 \neq \gamma_1$ which is beyond scope of this paper.

The stability branches of steady state convection, travelling waves and standing waves are summarized in Fig. 12 [2]. Here E_1 is total amplitude and defined as $E_1 = a_L^2 + a_R^2$. We do not distinguish between left travelling waves and right travelling waves. For rest state $E_1 = 0$, for travelling waves $E_1 = \frac{-\beta_1}{\gamma_1}$, for standing waves $E_1 = \frac{-2\beta_1}{\gamma_1+\delta_1}$. Travelling waves are supercritical if $\gamma_1 < 0$ and standing waves are supercritical if $\gamma_1 + \delta_1 < 0$. Fig. 12a is drawn for stable travelling wave conditions and Fig. 12b is drawn for stable standing wave conditions in (β_1, E_1)-plane. The symbols $(-,-)$ and $(+,-)$ in Figs. 12a and b indicate that both two roots of Jacobian are negative and atleast one root is positive among two roots. In Figs. 12a and b, travelling wave solution and standing wave solution bifurcate simultaneously from the steady sate solution ($\beta_1 \geqslant 0$ at this bifurcation point). In these Figs. 12a and b, steady state solution is stable for $\beta_1 < 0$ and unstable for $\beta_1 > 0$. These figures show that for $\beta_1 > 0$ both travelling waves and standing waves are supercritical. When travelling waves and standing waves bifurcate supercritically then atmost one solution among travelling waves and standing waves will be stable. Thus, for $\beta_1 > 0$ (Fig. 12a) travelling

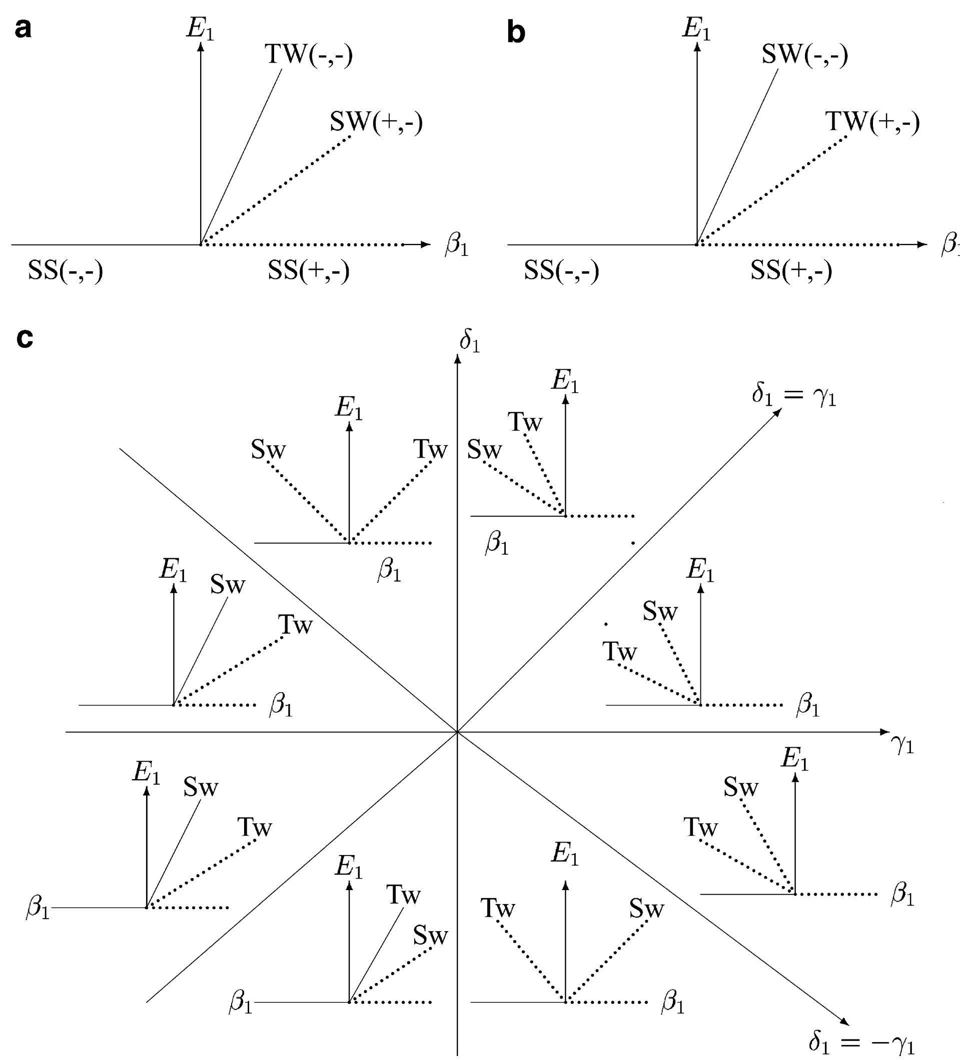

Fig. 12. (a), (b) and (c) are typical diagrams showing the stability of equilibrium solutions SS (steady state), SW (standing waves) and TW (travelling waves). On solid lines equilibrium solutions are stable and on dotted lines they are unstable.

waves are stable and (Fig. 12b) standing waves are stable. In more detail we reproduce results of the stability analysis of equilibrium solutions in Fig. 12c, which is plotted in (γ_1, δ_1)-plane. From this figure we can observe that travelling waves are subcritical for $\gamma_1 > 0$ and standing waves are subcritical for $\gamma_1 + \delta_1 > 0$.

The problem of thermohaline convection in rotating fluids, with periodic boundary conditions is studied by using a standard perturbation technique. Weakly nonlinear theory must be used to resolve which of standing or travelling waves will occur at the onset of convection. For each set of parameter values, the linear problem was solved to determine whether stationary or oscillatory mode becomes unstable first, as R_1 is increased. If it was found that the oscillatory mode becomes unstable, the coefficients Λ_o, Λ_1, Λ_2, Λ_3, Λ_4, Λ_5 were determined at the value of q_o that minimized R_{1o}, to investigate the stability of travelling or standing waves. In Fig. 13, we have showed the stability regions of standing waves and travelling waves in (Ta, R_2)-plane for $Pr = 0.025$, 0.1, 0.5. For $Pr = 0.025$, we get only stable standing waves at the onset of oscillatory convection. In the case of $Pr = 0.1$, 0.5 we get both travelling and standing waves are stable. This implies that at the onset if we get stable travelling waves (standing waves) then they loss their stability to standing waves (travelling waves) soon after the initial bifurcation as Ta increases for a fixed R_2 in (Ta, R_2)-plane. The stable regions of both travelling and standing waves increases as Pr increases.

Now we will give exact solutions for Eqs. (5.18) and (5.19) when $\gamma_1 = \delta_1$. Substituting

$$a_L(t) = r(t)\cos\psi(t) \quad \text{and} \quad a_R(t) = r(t)\sin\psi(t) \tag{5.21}$$

into Eqs. (5.18) and (5.19), we get

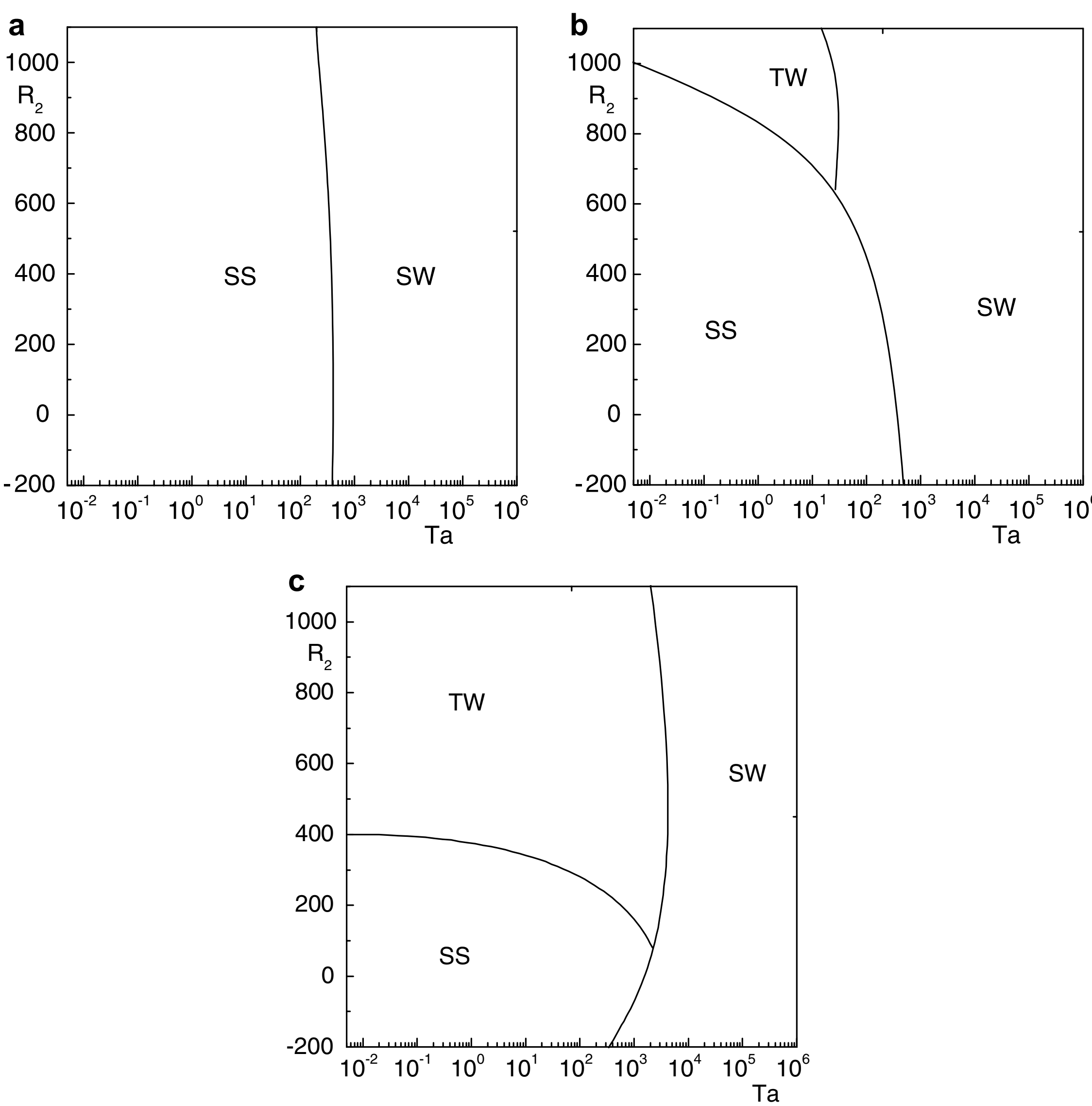

Fig. 13. Stability regions of steady state (SS), standing waves (SW) and travelling waves (TW) are plotted at the onset of oscillatory convection for $L = 0.1$, (a) $Pr = 0.025$, (b) $Pr = 0.1$, (c) $Pr = 0.5$.

$$\frac{dr}{dt} = r(\beta_1 + r^2\mathscr{P}), \tag{5.22}$$

$$\frac{d\psi}{dt} = \frac{r^2}{4}(\delta_1 - \gamma_1)\sin 4\psi, \tag{5.23}$$

where $\mathscr{P} = \gamma_1(\sin^4\psi + \cos^4\psi) + 2\delta_1 \sin^2\psi\cos^2\psi$. From the transformation (5.21), we get left travelling waves at $\psi = \psi_o = 0$, right travelling waves at $\psi = \psi_o = \pi/2$ and standing waves at $\psi = \psi_o = \pi/4$. At $\gamma_1 = \delta_1$, Eq. (5.23) gives $\psi = \psi_o =$ constant. Now Eq. (5.22) becomes

$$\frac{dr}{dt} = r(\beta_1 + r^2\gamma_1). \tag{5.24}$$

The equilibrium solutions are supercritical when $\beta_1 > 0$ and $\gamma_1 < 0$.

Case 1: For $\beta_1 > 0$ and $\gamma_1 < 0$, Eq. (5.24) gives the solution

$$r(t) = \frac{\sqrt{-\beta_1/\gamma_1}}{\left[1 - \left(\frac{\beta_1/\gamma_1}{r_o^2} + 1\right)e^{-2\beta_1 t}\right]^{\frac{1}{2}}}, \tag{5.25}$$

where $r_o = r(0)$. Clearly the solution $r(t) \to \sqrt{-\beta_1/\gamma_1}$ as $t \to \infty$.

Case 2: For $\beta_1 < 0$, say $\beta_1 = -k^2$ and $\gamma_1 < 0$, Eq. (5.24) gives the solution

$$r(t) = \frac{k/\sqrt{-\gamma_1}}{\left[-1 + \left(\frac{-k^2/\gamma_1}{r_o^2} + 1\right)e^{2k^2 t}\right]^{\frac{1}{2}}}. \tag{5.26}$$

The solution (5.26) showing the subcritical stable behavior. For the case $\beta_1 < 0$, say $\beta_1 = -k^2$ and $\gamma_1 > 0$, Eq. (5.24) has the solution

$$r(t) = \frac{k/\sqrt{\gamma_1}}{\left[1 + \left(\frac{k^2/\gamma_1}{r_o^2} - 1\right)e^{2k^2 t}\right]^{\frac{1}{2}}}. \tag{5.27}$$

The solution (5.27) shows that the nonlinear effects produce a subcritical instability if the amplitude exceeds the threshold $r_o > k/\sqrt{\gamma_1}$, otherwise we get subcritical stable state.The solutions of Landau equation (5.24) show that a supercritical stable behavior and a subcritical unstable behavior under the suitable conditions.

6. Conclusions

In this paper the stability of thermohaline convection in rotating fluid has been investigated. By eliminating the thermal Rayleigh number R_1 from $E = 0$ and $D = 0$, we get the value of $R_2 = R_{2c}$ given by Eq. (3.11). We have also obtained the values of Takens–Bogdanov bifurcation points and co-dimension two points by plotting graphs of neutral curves corresponding to stationary and oscillatory convection for different values of physical parameters relevant to thermohaline convection in rotating fluid. From Eq. (3.8), we get two Takens–Bogdanov bifurcation points for $R_2 > 0$, while from Eq. (3.22) we get two Takens–Bogdanov bifurcation points for both $R_2 < 0$ and $R_2 > 0$. In this problem for $L = 1$, $\mathscr{L}w = 0$ gives a cubic polynomial equation in p, from which we get an analytical expression at co-dimension two point given by Eq. (3.31). This Eq. (3.31) is same as Eq. (A_4) given in Appendix by Pearlistien [6]. For $L \neq 1$, we get oscillatory convection for both $Pr < 1$ and $Pr > 1$. We have considered only the physically realistic case of $L < 1$. We get co-dimension three bifurcation point at $R_2 = R_{2c}^*$ by eliminating Ta and R_1 from equations $E = 0$, $D = 0$ and $C = 0$, given by Eq. (3.23).

We have derived two-dimensional Landau–Ginzburg equation (4.11) at the onset of supercritical pitchfork bifurcation. For $R_2 < R_{2c}$, $\lambda_o > 0$ and we get Eq. (4.11). For $\lambda_o = 0$, we get $R_2 = R_{2c}$ which corresponds to Takens–Bogdanov bifurcation point given by Eq. (3.11) at $q = q_{sc}$. Near the Takens–Bogdanov bifurcation point the conducting state becomes unstable against both stationary and oscillatory mode, i.e., the real parts of two eigenvalues pass through zero nearly simultaneously. This violets the assumption made for deriving the amplitude equation (4.11) and amplitude equations (5.9a) and (5.9b). A new amplitude equation, which is second order in time, has to be used near the Takens–Bogdanov bifurcation point. This amplitude equation (which is second order in time) is valid near the Takens–Bogdanov bifurcation point includes Eqs. (5.9a) and (5.9b) as special cases, leading to relations between the respective coefficients. λ_2 is always positive.

Landau–Ginzburg equation (4.11) is valid only for supercritical bifurcation ($\lambda_3 > 0$). $\lambda_3 = 0$ corresponds to the tricritical bifurcation point. By using Eq. (4.13), we have obtained conditions for long wave-length instabilities viz. Eckhaus and zigzag instabilities. We have also calculated Nusselt number by dropping t-dependence from Eq. (4.13). To study the effect of physical parameters on heat transport it is necessary that $\lambda_3 > 0$.

We have derived one-dimensional nonlinear coupled Landau–Ginzburg type equations (5.9a) and (5.9b) at the onset of supercritical Hopf bifurcation by using two time scales. The discussion related to equilibrium solutions viz., steady state, travelling waves and standing waves are independent of boundary conditions. If both travelling waves and standing waves bifurcate supercritically, the one with larger E_1 will be stable. $E_1 = 0$ for steady state solution. Fig. 12a and b are typical diagrams correspond to stability conditions of travelling waves and standing waves respectively. From Fig. 12c, it is evident that in $\gamma_1 > 0$, $\gamma_1 + \delta_1 > 0$ regions both travelling waves and standing waves are unstable and in $\gamma_1 < 0$, $\gamma_1 + \delta_1 < 0$ regions either travelling waves or standing waves are stable. We have also studied the stability regions of travelling waves and standing waves in (Ta, R_2)-plane and observed that when Pr increases then we get both stable standing waves and travelling waves. We have obtained the exact analytical solutions when $\gamma_1 = \delta_1$, for travelling waves and standing waves. The analytical solution of Landau problem (5.24) gives the supercritical stable travelling waves and standing waves for $\beta_1 > 0, \gamma_1 < 0$ and subcritical unstable travelling waves and standing waves for $\beta_1 < 0,\ \gamma_1 < 0$. We can have similar analytical discussion from Landau equations (5.18) and (5.19) to travelling waves ($a_L = 0$ or $a_R = 0$) and standing waves ($a_L = a_R$).

References

[1] A. Arneodo, P.H. Coullet, E.A. Spiegel, The dynamics of triple convection, Geophys. Astrophys. Fluid Dynam. 31 (1985) 1.

[2] E. Knobloch, Oscillatory convection in binary mixtures, Phys. Rev. A 34 (1986) 1538.

[3] R.C. Kloosterziel, G.F. Carnevale, Closed-form linear stability conditions for rotating Rayleigh–Benard convection with rigid, stress-free upper and lower boundaries, J. Fluid Mech. 480 (2003) 25.

[4] P.C. Matthews, A.M. Rucklidge, Travelling and standing waves in magnetoconvection, Proc. R. Soc. Lond. A 441 (1993) 649.

[5] A.C. Newell, J.A. Whitehead, Finite band width, finite amplitude convection, J. Fluid Mech. 38 (1969) 279.

[6] A.J. Pearlstein, Effect of rotation on the stability of a doubly diffusive fluid layer, J. Fluid Mech. 103 (1981) 389.

[7] S.G. Tagare, Nonlinear stationary magnetoconvection in a rotating fluid, J. Plasma Phys. 58 (1997) 395.

[8] S.G. Tagare, Y. Rameshwar, Magnetoconvection in rotating stars, Astrophys. Space Sci. 284 (2002) 983.

[9] G. Veronis, On finite amplitude instability in thermohaline convection, J. Marine Res. 23 (1965) 1.